

Review

Advancing electrochemical impedance analysis through innovations in the distribution of relaxation times method

Adeleke Maradesa,¹ Baptiste Py,¹ Jake Huang,² Yang Lu,³ Pietro Iurilli,⁴ Aleksander Mrozinski,⁵ Ho Mei Law,⁶ Yuhao Wang,¹ Zilong Wang,¹ Jingwei Li,⁶ Shengjun Xu,⁶ Quentin Meyer,⁷ Jiapeng Liu,⁸ Claudio Brivio,⁹ Alexander Gavrilyuk,¹⁰ Kiyoshi Kobayashi,¹¹ Antonio Bertei,¹² Nicholas J. Williams,^{13,14} Chuan Zhao,⁷ Michael Danzer,¹⁵ Mark Zic,¹⁶ Phillip Wu,¹⁷ Ville Yrjänä,¹⁸ Sergei Pereverzyev,¹⁹ Yuhui Chen,²⁰ André Weber,²¹ Sergei V. Kalinin,^{22,23} Jan Philipp Schmidt,²⁴ Yoed Tsur,^{25,26} Bernard A. Boukamp,²⁷ Qiang Zhang,³ Miran Gaberšček,²⁸ Ryan O’Hayre,² and Francesco Ciucci^{1,6,*}

SUMMARY

Electrochemical impedance spectroscopy (EIS) is widely used in electrochemistry, energy sciences, biology, and beyond. Analyzing EIS data is crucial, but it often poses challenges because of the numerous possible equivalent circuit models, the need for accurate analytical models, the difficulties of nonlinear regression, and the necessity of managing large datasets within a unified framework. To overcome these challenges, non-parametric models, such as the distribution of relaxation times (DRT, also known as the distribution function of relaxation times, DFRT), have emerged as promising tools for EIS analysis. For example, the DRT can be used to generate equivalent circuit models, initialize regression parameters, provide a time-domain representation of EIS spectra, and identify electrochemical processes. However, mastering the DRT method poses challenges as it requires mathematical and programming proficiency, which may extend beyond experimentalists' usual expertise. Post-inversion analysis of DRT data can be difficult, especially in accurately identifying electrochemical processes, leading to results that may not always meet expectations. This article examines non-parametric EIS analysis methods, outlining their strengths and limitations from theoretical, computational, and end-user perspectives, and provides guidelines for their future development. Moreover, insights from survey data emphasize the need to develop a large impedance database, akin to an impedance genome. In turn, software development should target one-click, fully automated DRT analysis for multidimensional EIS spectra interpretation, software validation, and reliability. Particularly, creating a collaborative ecosystem hinged on free software could promote innovation and catalyze the adoption of the DRT method throughout all fields that use impedance data.

INTRODUCTION

Electrochemical impedance spectroscopy (EIS)¹ is a characterization technique widely used in the electrochemistry,² energy storage and conversion,³ electrocatalysis,⁴ and biosciences⁵ sectors due to its non-invasiveness, ease of use, and

CONTEXT & SCALE

Electrochemical impedance spectroscopy (EIS) is a key tool across various scientific disciplines, including energy sciences, chemistry, and biology, enabling the analysis of electrochemical systems. However, conventional methods for interpreting EIS data are often complex and model dependent. The distribution of relaxation times (DRT) offers a non-parametric approach that simplifies the interpretation process by providing a timescale interpretation of EIS data. This article provides a comprehensive review of current methods for DRT inversion. Additionally, a survey of practitioners highlights key challenges in the field. The findings underscore the need for standardized DRT analysis and benchmarks, as well as the development of automated analysis tools. These advancements would improve the usability and interpretability of EIS data. Ultimately, implementing these improvements could not only propel the field forward but also expand the application of DRT in scientific research by



capability to probe a wide range of timescales. To interpret EIS spectra, models are needed.⁶ For that purpose, equivalent circuits or physical models are usually used.⁷ However, models based on equivalent circuit analogs may be non-unique. This means that various circuits with possibly different structures can exhibit the same impedance response, hindering physical interpretation.⁸ Alternatively, physical models can be used but are system-specific and difficult to implement.⁹ In the last two decades, non-parametric models, such as the distribution of relaxation times (DRT), have emerged as promising solutions to overcome these challenges.¹⁰ The DRT approach underpins the determination of a timescale distribution, which is obtained by solving the following Fredholm integral equation for the latent distribution $\gamma(\log \tau)$ ¹¹:

$$Z_{\text{DRT}}(f) = R_\infty + i2\pi fL_0 + \int_{-\infty}^{+\infty} \frac{\gamma(\log \tau)}{1+i2\pi f\tau} d \log \tau \quad (\text{Equation 1})$$

where $Z_{\text{DRT}}(f)$ ¹² is the impedance obtained with the DRT model, $\gamma(\log \tau)$ ¹³ is the actual DRT, and τ , f , R_∞ , and L_0 are the timescale, frequency, ohmic resistance, and inductance, respectively. In its basic form, the DRT model (Equation 1) assumes that the impedance is closely connected to Voigt circuits. This loosely involves an infinite series of parallel resistor-capacitor elements, where $\gamma(\log \tau)$ is the distribution of resistances associated with a given timescale.^{7,14} As shown in Figures 1 and 2, starting from EIS data, $\gamma(\log \tau)$ can be obtained by mapping the impedance data into a distribution of the time constants of the system under study.^{15,16}

The DRT model offers several benefits. Its generality requires only a basic understanding of the EIS spectra being analyzed, making it highly accessible to non-experts. This eliminates the need for constructing equivalent circuits or developing *ad hoc* physical models, offering a more straightforward interpretation compared to raw EIS data. Its simplicity lies in representing individual relaxation processes as peaks in the distribution, enhancing the understanding of impedance spectra. Furthermore, when discretized, the DRT model is linear, implying that finding an approximation of $\gamma(\log \tau)$ using (Equation 1) by regressing a single EIS spectrum¹⁷ may require only setting up a relatively straightforward quadratic optimization problem,¹⁸ which can be solved in a few milliseconds even with an entry-level laptop computer.¹⁹ Applications of the DRT framework have ranged widely, from the determination of equivalent circuits to the analysis of processes occurring in batteries,^{20–23} fuel cells,^{15,24,25} supercapacitors,²⁶ and even agricultural plant products.²⁷ The DRT method has recently been employed to analyze multiple spectra,²⁸ offering benefits over an equivalent circuit approach by facilitating unified data handling, circumventing the nonlinear challenges of circuit fitting, and enabling more direct analysis. Unlike an equivalent circuit model, the DRT does not rely on speculative assumptions about the processes. Instead, it extracts timescales and resistances corresponding to different electrochemical processes directly from EIS data, without needing a pre-determined physical model or arbitrary circuit. The DRT method has been used to identify peaks (representing electrochemical processes) and guide the development of physicochemically meaningful equivalent circuits.^{29,30} In particular, the parameters obtained from DRT can serve as initial values for subsequent EIS spectra regression.³⁰ Additionally, this method can be used to assess data quality through the analysis of the Kramers-Kronig transform.³¹ Interestingly, the DRT can also accelerate impedance acquisition by enabling the integration of time-domain and frequency data.³²

Despite its promise, the DRT framework still has shortcomings. First, the deconvolution of (an approximation of) $\gamma(\log \tau)$ using (Equation 1)³³ requires solving an

making it accessible to a broader range of researchers, including those without specialized expertise in programming or statistics.

¹Department of Mechanical and Aerospace Engineering, The Hong Kong University of Science and Technology, Hong Kong, Hong Kong SAR, China

²Metallurgical and Materials Engineering, Colorado School of Mines, Golden, CO 80401, USA

³Beijing Key Laboratory of Green Chemical Reaction Engineering and Technology, Department of Chemical Engineering, Tsinghua University, Beijing, China

⁴Green Energy Storage, 38123 Trento, Italy

⁵Department of Manufacturing and Production Engineering, Faculty of Mechanical Engineering and Ship Technology, Institute of Machine and Materials Technology, Gdańsk University of Technology, Gdańsk, Poland

⁶Electrode Design for Electrochemical Energy Systems, University of Bayreuth, Bayreuth, Germany

⁷School of Chemistry, University of New South Wales, Sydney, NSW Australia

⁸School of Advanced Energy, Sun Yat-Sen University, Shenzhen, China

⁹Sustainable Energy Center, CSEM 2002 Neuchâtel, Switzerland

¹⁰Interdisciplinary Faculty of Science and Engineering, Shimane University, Matsue, Japan

¹¹Centre for Electronic and Optical Materials, National Institute for Materials Science, Tsukuba, Japan

¹²Department of Civil and Industrial Engineering, University of Pisa, Pisa, Italy

¹³Department of Materials, Imperial College London, Exhibition Road, London SW7 2AZ, UK

¹⁴Department of Chemical Engineering, Massachusetts Institute of Technology, Cambridge, MA 02139, USA

¹⁵Electrical Energy Systems, University of Bayreuth, Bayreuth, Germany

¹⁶Ruder Boskovic Institute, Zagreb, Croatia

¹⁷Department of Materials and Minerals Resources Engineering, National Taipei University, Taipei, Taiwan

¹⁸Laboratory of Molecular Science and Engineering, Faculty of Science and Engineering, Johan Gadolin Processing Chemistry Centre, Åbo Akademi University, Turku (Åbo), Finland

¹⁹Johann Radon Institute for Computational and Applied Mathematics, Linz, Austria

Continued

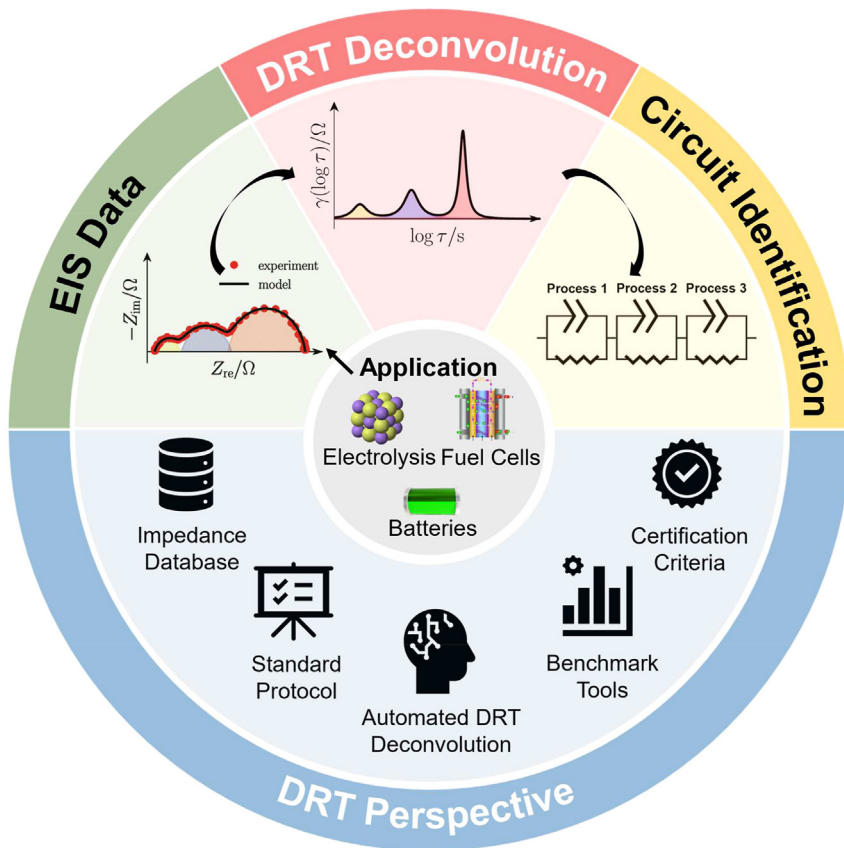


Figure 1. DRT application and perspective for expanding the DRT field

ill-posed problem that depends strongly on experimental errors.⁶ Second, DRT feature attribution is still challenging due to the emergence of spurious peaks and related difficulties with associating peaks to specific physical processes.^{10,34} Third, the DRT method (in its naive form) is generally unsuitable for systems with blocking electrodes, such as those encountered in batteries. In fact, (Equation 1) implies that for $f \rightarrow 0$ the impedance has a finite value $R_\infty + \int_{-\infty}^{+\infty} \gamma(\log \tau) d \log \tau$.³⁵ In devices featuring blocking electrodes, such as lithium-ion batteries, the impedance approaches infinity as the frequency approaches zero. This poses challenges, especially when dealing with multiple EIS spectra datasets or in cases of limited theoretical understanding.²⁸

To overcome these issues, there is a need for dedicated software that is both reliable and user-friendly. Progress in this area requires establishing standardized practices and benchmarking methods (Figure 1). These steps are essential when testing DRT software so that the corresponding analysis is reproducible and reliable.³⁶ Importantly, end-users should face reduced mathematical and computational complexity while gaining improved interpretability of the results obtained. For example, DRT analysis could be coupled with automatic peak deconvolution and classification.³⁷ Yet, the path to overcome these challenges is still largely uncharted. It necessitates the creation of novel, rigorously tested methods as well as user-friendly software code with specific target features, including data quality assessment, automation of DRT deconvolution, simplicity, versatility, and robustness (Figure 1). Although the DRT deconvolution is a regularization problem, the regularization parameter,

²⁰School of Science and Engineering, Nanjing Tech. University, Nanjing, China

²¹Institute for Applied Materials – Electrochemical Technologies (IAM-ET), Karlsruhe Institute of Technology (KIT), Karlsruhe, Germany

²²Department of Materials Science and Engineering, University of Tennessee, Knoxville, TN 37996, USA

²³Physical Science Division, Pacific Northwest National Laboratory, Richland, WA 99354, USA

²⁴Systems Engineering for Electrical Energy Storage, University of Bayreuth, Bayreuth, Germany

²⁵Technion, Israel Institute of Technology, Department of Chemical Engineering, Haifa, Israel

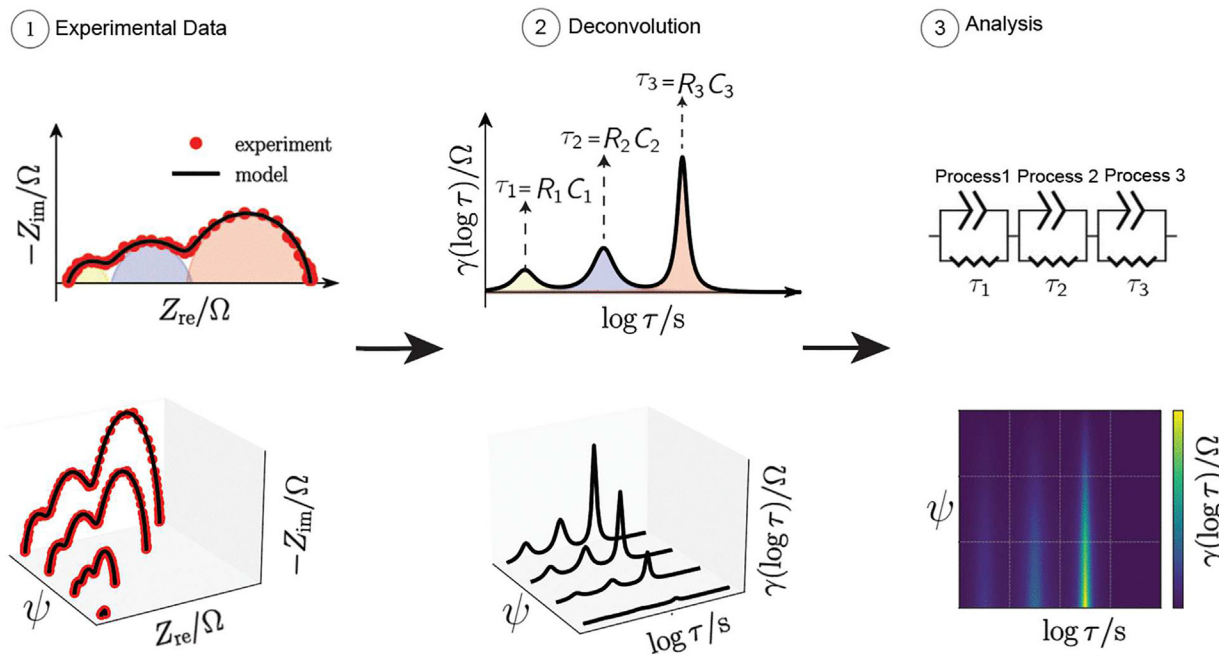
²⁶Grand Technion Energy Program, Technion, Israel Institute of Technology, Haifa, Israel

²⁷University of Twente, Enschede, the Netherlands

²⁸National Institute of Chemistry, Ljubljana, Slovenia

*Correspondence:
francesco.ciucci@uni-bayreuth.de

<https://doi.org/10.1016/j.joule.2024.05.008>



Frequency domain with semicircles corresponding to specific processes

Associating DRT peaks to specific processes

Figure 2. Starting with EIS data, the DRT is deconvolved, which results in the identification of timescales, and subsequent analysis allows the identification of the corresponding electrochemical processes

λ , is usually manually provided.¹⁷ However, the choice of λ can be automated using, for example, the cross-validation³⁸ or the L-curve,³⁹ and the self-tuning Levenberg-Marquardt approach.⁴⁰ This article offers a comprehensive examination of non-parametric DRT methods and outlines future directions, informed by survey data, which aim to support a continuous improvement of the DRT methods while broadening their applicability.

DRT WORKFLOW AND APPLICATIONS

Before exploring the DRT-specific methods, we offer an overview of the standard workflow of EIS analysis via the DRT method (Figure 2). Starting from EIS data consisting of a single spectrum or multiple spectra dependent on some experimental state, the DRT is deconvolved (deconvolution methods are detailed in section **DRT-based deconvolution and analysis methods**)^{28,41} by regressing the DRT model (Equation 1) against experimental data (see panel 1 of Figure 2). DRT deconvolution allows extracting the timescale characteristics of an electrochemical system by directly inspecting $\gamma(\log \tau)$ (panel 2 of Figure 2). For example, by examining $\gamma(\log \tau)$ across different experimental states, shifts in the system's characteristic response due to varying conditions (for fuel cells, these could be oxygen partial pressure or temperature, while for batteries, these can be state of charge or state of health) can be directly assessed. This insight can be leveraged in various ways, for instance, to determine an appropriate equivalent circuit^{6,42} and to subsequently quantify key physical parameters like charge-transfer resistances, double-layer capacitances, etc. (see Ivers-Tiffée and Webér²⁰ for the historical overview of DRT analysis in the EIS field). Below, we describe specific examples, from batteries and fuel cells, where the DRT has been used to gain insights from experimental data.

The DRT method has proven highly useful in analyzing secondary (rechargeable) batteries, with applications in both academic research and industry.⁴³ DRT peak attribution has been instrumental in detecting the timescales of various processes, including intercalation,^{44–46} solid electrolyte interface formation,⁴⁷ and ionic conduction at grain boundaries.^{48–51} It is applicable to various battery systems, including solid-state and lithium-sulfur batteries, and has revealed new mechanisms such as the formation of anodic lithium voids²² and polysulfide reactions.⁵² In electrode design, the DRT method has also been used to identify the interfacial surface charge mechanism, which contributes to the enhanced battery capacity at high current density. This insight has been useful for selecting advanced lithium-ion battery anode materials.⁵³

Combining DRT with EIS allows for efficient batch processing and visualization of changes in anodic⁵⁴ and cathodic interfacial evolution,²³ which is otherwise challenging with other methods. In the industry, DRT methods have been used to efficiently extract key kinetic information, crucial for assessing commercial batteries, including their state of health⁵⁵ and state of charge,⁵⁶ with applications in the fields of portable electronic devices and electric mobility. Integrating the DRT and artificial intelligence (AI) is promising for battery diagnosis,⁵⁷ lifespan estimation,⁵⁸ and understanding retired batteries' echelons.⁵⁷

The DRT plots (in panel 2 of Figure 2) identify distinct peaks that can be attributed to specific electrochemical processes, offering richer insights compared with the Nyquist plots. These insights can be leveraged to accurately distinguish processes with overlapping time constants, particularly in batteries with diverse kinetic processes (e.g., lithium-sulfur batteries), which are challenging to analyze based on the Nyquist presentation.¹⁰ In many *in situ* impedance results, manual simulations are notoriously time-consuming and affected by inherent errors. On the other hand, DRT can batch-process EIS data while ensuring both accurate and efficient results.¹⁰

The open-system nature of fuel cells, capable of achieving steady-state operation, makes them particularly well suited for DRT analysis, even at low frequencies. In solid oxide fuel cells (SOFCs) and proton exchange membrane fuel cells (PEMFCs), the DRT method has been used to distinguish electrochemical processes and identify degradation mechanisms.^{29,59–65} It helps to elucidate the effects of material modifications on the kinetically sluggish oxygen reduction¹⁵ and oxygen evolution reactions,⁶⁶ thereby aiding the selection of suitable materials and cell designs.^{67–69} DRT methods have been instrumental in enhancing the interpretability of impedance data. For example, its peak-based analysis can separate gas diffusion and proton transfer impedances, particularly at low and high current densities, respectively, which can be valuable for fuel cell fault diagnosis and durability.⁷⁰ Compared with the conventional impedance analysis, the DRT has been used to determine the type of frequency response of different electrochemical processes occurring in SOFCs, guiding equivalent circuit selection and revealing many processes (e.g., oxygen reduction at a particular temperature, gas diffusion, and reaction rate).⁷¹ In addition, DRT analysis enables a clear representation of an equivalent circuit, revealing the distinct contributions of fitting elements, which consequently benefit the analysis of complex impedance spectra.⁷² The DRT's peak area can directly reflect the polarization value of the corresponding electrochemical processes while allowing deconvolution of each peak, representing proton diffusion, anode reaction of hydrogen adsorption/dissociation, proton formation, and cathode surface oxygen reactions.^{73,74} By contrast, the traditional impedance-based analytic methods, such as Nyquist analysis, can only identify the total polarization without clearly distinguishing the contributions from the various components.^{73,75}

DRT can be used to analyze battery and fuel cell electrodes. However, challenges may arise when the timescales of the electrode overlap. For instance, multiple peaks related to charge transfer, charge- and gas-transport (in the transmission line, Warburg-type gas diffusion, or Gerischer models) might be significantly affected.^{76,77} For water electrolyzers, the DRT approach enables the deconvolution of the ion transfer, charge transfer, and mass-transport mechanisms of the oxygen and hydrogen evolution reactions.⁷⁸

SURVEY

Despite their rising popularity and range of applications, DRT methods must be further expanded and standardized. Although DRT methods are gaining popularity and have a broad application spectrum, there is a pressing need for more user-focused improvements. Therefore, we developed a survey that integrates the theoretical and practical aspects of DRT to determine user challenges and needs. By linking theory with application, this survey highlights urgent user-centered requirements, providing vital data for the EIS community to develop impactful solutions.

We developed a bilingual survey to reach a wider spectrum of users and gather experts' feedback. The survey was distributed to 1,850 scientists who have either authored or cited key DRT papers, sourcing their contact information via Google Scholar through Python's scholarly package.⁷⁹ Concurrently, a Chinese version of the survey was shared with 930 scientists working on fuel cells and batteries. The data revealed that most respondents work on fuel cells (45%), followed by batteries (18%) and electrolyzers (15%) (Figure S1B and Table S3 in Ciucci et al.⁸⁰), and use the DRT method to characterize electrode-electrolytes interfaces (31%), identify reaction mechanisms (29%), or evaluate battery performance (20%) (Figure 3B and Table S4 in Ciucci et al.⁸⁰). Although 70% of the respondents expressed satisfaction with current DRT methods, they also identified limitations, including the lack of physical interpretability (45%) and a limited connection with underlying mechanisms (37%) (Figures 3B and S2 and Table S1 in Ciucci et al.⁸⁰).

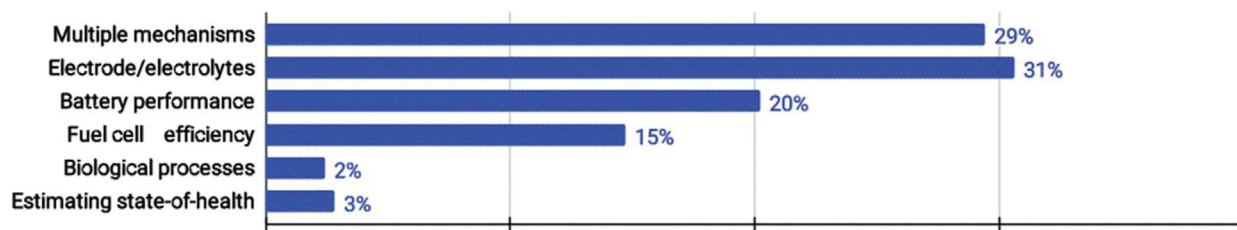
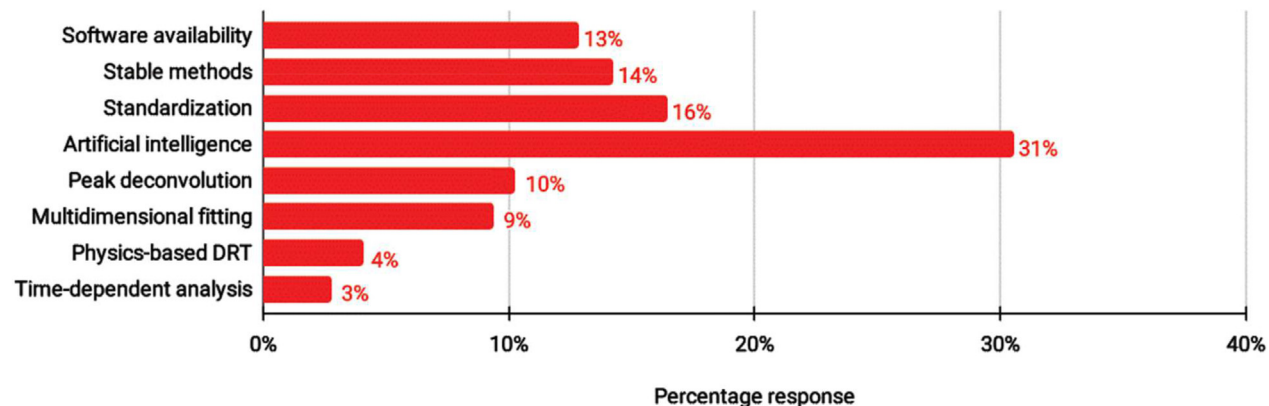
Respondents proposed enhancements such as automated DRT frameworks correlating peaks with specific electrochemical processes (39%, Figure 3A). They also suggested automating DRT deconvolution (37%, Figure 3A), including data assimilation, deconvolution, and validation. Furthermore, respondents emphasized the need for timescale separation (20%) and standardized validation tests (16%, Figure 3C) of software to certify reproducible DRT outputs. The limited use of DRT in biology and medicine (58%, Figure S2A in Ciucci et al.⁸⁰) suggests potential expansion into these areas.

Caution should be exercised when interpreting the results of this survey due to limitations such as sampling bias, untraced DRT user demographics, anonymity constraints, and low response rates (4.0% and 6.0% for the English and Chinese versions, respectively). Despite these limitations, the survey serves as a preliminary indicator of community needs and provides a foundation for future research, including creating more reliable surveys to further guide DRT development. More details about the survey can be found elsewhere.⁸⁰

DRT-BASED DECONVOLUTION AND ANALYSIS METHODS

DRT deconvolution

DRT deconvolution requires estimating $\gamma(\log \tau)$ from measured impedance values at discrete frequencies (i.e., an impedance spectrum). Determining $\gamma(\log \tau)$ from

A What functionalities do you expect new DRT methods/software to possess?**B How has DRT analysis contributed to the understanding of materials and systems?****C What can still be improved regarding DRT methods/software?****Figure 3. Surveying DRT methods: Expectations, impact, and future improvement**

Bar chart showing the responses related to (A) the functionalities expected from new DRT methods/software, (B) how DRT analysis has contributed to the understanding of materials and systems, and (C) the aspects of DRT methods/software needing further improvement.

(Equation 1) requires discretizing the DRT function within a certain approximation space^{14,28,81–87}; typically $\gamma(\log \tau)$ is assumed to be a continuous function. As shown in Figure 4, many techniques can be used to perform DRT deconvolution, each of which defines a different approach to the inversion problem. These include regularized regression and collocation,^{14,40,88} genetic algorithms⁸⁶ and genetic programming,^{89,90} Monte Carlo,⁹¹ deep neural networks,^{28,92} Fourier transforms,^{93,94} Bayesian methods,^{18,95} Gaussian processes (GPs),^{77,81} and methods combining EIS and time-domain data.³² Regularized regression is effective for multidimensional spectra but challenging for discontinuous DRTs. For example, naive regularized regression struggles to accurately recover models like Gerischer, piecewise constant, and even parallel resistor-capacitor elements. Additionally, since regularized regression is a point estimator, it complicates the quantification of uncertainty of the recovered DRT.⁹⁶ Genetic algorithms model the DRT as a distribution, while genetic programming searches for the best model comprising several peaks chosen from a given library.^{86,89} However, both methods suffer from slow computational convergence. Moreover, genetic programming necessitates the inclusion of polarization

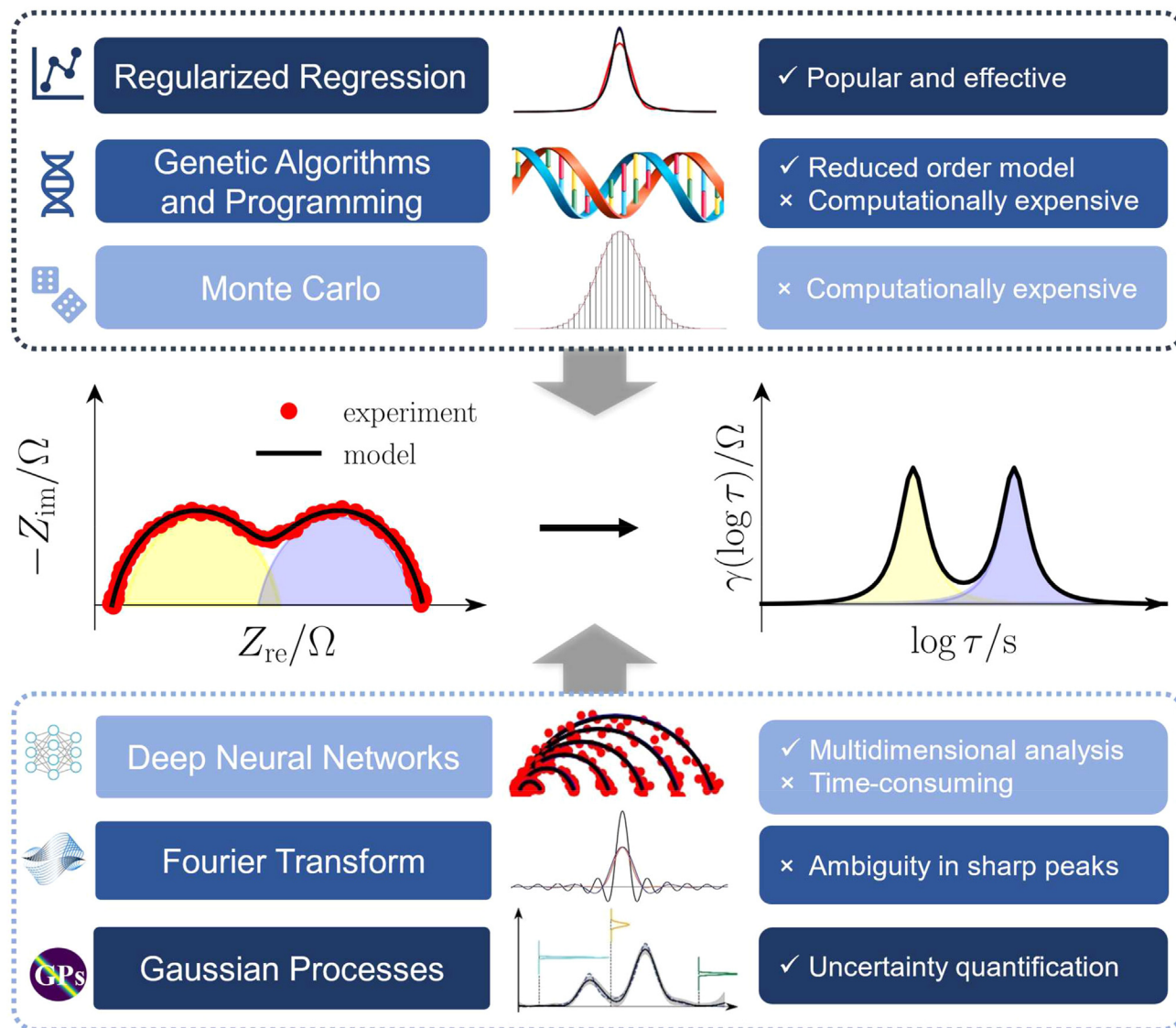


Figure 4. Different deconvolution methods (in inverse problem) used to develop various DRT frameworks and software

Reproduced with permission from Quattrocchi et al.,²⁸ Maradesa et al.,³⁸ Baral and Tsur,⁹⁷ Bello et al.,⁹¹ Boukamp,⁹³ and Maradesa et al.⁹⁸

processes within a set library, potentially leading to inaccurate results should specific processes be absent.

Monte Carlo techniques have also been used to obtain the DRT but are computationally expensive.⁹⁹ Although deep neural networks can handle unstructured data and be used for prediction, they rely on numerous hyperparameters and require time-consuming training.^{28,100} The Fourier transform can accurately identify peaks but may struggle with sharp and asymmetric peaks, as well as sparse EIS data points.^{93,94} Bayesian methods have evolved from the understanding that regularized regression can be interpreted from a Bayesian perspective. These methods consider the DRT and (potentially) the regularization parameter, λ , as random variables. As a result, they retain the properties of regularized regression, provide uncertainty on the DRT, can manage discontinuous distribution,⁹⁵ can be used to handle data outliers,¹⁰¹ and can, in principle, be extended to resolve edge

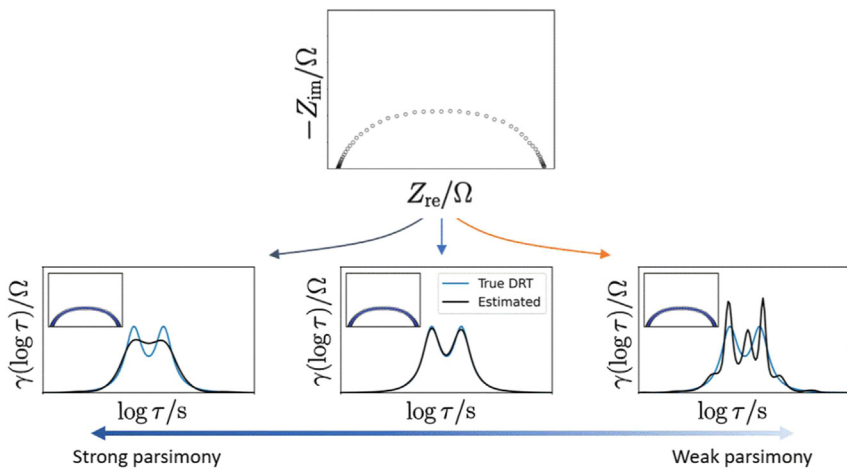


Figure 5. Starting from EIS data, the DRT is deconvolved based on the principle of parsimony
Reproduced with permission from Huang.¹⁰⁵

effects.¹⁰² Bayesian methods prioritize simpler solutions, aligning more closely with the principle of parsimony,^{37,103,104} which states that the most credible solution is the simplest one that accurately describes the data^{37,101} (Figure 5). However, this approach necessitates the optimization of numerous hyperparameters.^{18,101} GPs quantify uncertainty in DRT recovery, are robust against noise, and allow evidence maximization. However, their application in analyzing large EIS datasets may prove computationally inefficient due to poor computational scalability.^{77,98} Combining EIS and time-domain data offers faster EIS acquisition but requires careful management of error propagation to maintain accuracy.^{31,32} The sections below illustrate these methods, highlighting their main trait and use for DRT deconvolution.

Regularized regression

Regularized regression is nowadays one of the most widely used approaches for DRT deconvolution. It minimizes the sum of squared residuals to yield a discretized version of $\gamma(\log \tau)$ ^{14,106}:

$$\mathbf{x}(\log \tau) = \underset{\mathbf{x}^* \geq 0}{\operatorname{argmin}} \left(\|\boldsymbol{\Omega}_{\text{re}}(\mathbf{Z}_{\text{exp,re}} - \mathbf{A}_{\text{re}}\mathbf{x}^*)\|_2^2 + \|\boldsymbol{\Omega}_{\text{im}}(\mathbf{Z}_{\text{exp,im}} - \mathbf{A}_{\text{im}}\mathbf{x}^*)\|_2^2 + P(\mathbf{x}^*) \right) \quad (\text{Equation 2})$$

where \mathbf{x} is the DRT discretized at a set of N collocation points $\log \tau = (\log \tau_1, \log \tau_2, \dots, \log \tau_N)^T$, $\boldsymbol{\Omega}_{\text{re}} = \text{diag}(\sqrt{w_{\text{re},1}}, \sqrt{w_{\text{re},2}}, \dots, \sqrt{w_{\text{re},M}})$, and $\boldsymbol{\Omega}_{\text{im}} = \text{diag}(\sqrt{w_{\text{im},1}}, \sqrt{w_{\text{im},2}}, \dots, \sqrt{w_{\text{im},M}})$ are diagonal matrices containing the weights $w_{\text{re},n}$ and $w_{\text{im},n}$ with $n = 1, 2, \dots, M$, for the real and imaginary parts of the impedance, respectively, $\mathbf{Z}_{\text{exp,re}}$ and $\mathbf{Z}_{\text{exp,im}}$ are the vectors of the real and imaginary parts of the impedance measured at M frequencies, respectively, \mathbf{A}_{re} and \mathbf{A}_{im} are two matrices discretizing (Equation 1), $\|\cdot\|_2$ is the Euclidian norm, and $P(\mathbf{x}^*)$ is a penalty term. It should be noted that before solving (Equation 2), it is crucial to compute \mathbf{A}_{re} and \mathbf{A}_{im} . This computation involves solving integrals, typically necessitating discretization. However, the adoption of specific functions^{16,88} allows for the analytical computation of these matrices' components, thus leading to no integration errors. Well-established numerical packages, such as CVXOPT,¹⁰⁷ and the Levenberg-Marquardt algorithm,^{108,109} among others,¹¹⁰ can be used to solve (Equation 2). The penalty term $P(\mathbf{x}^*)$ in (Equation 2) strongly influences the solution. For ridge regression (also referred to as Tikhonov regularization), $P(\mathbf{x}^*) = \lambda \|\mathbf{L}\mathbf{x}^*\|_2^2$ where $\lambda \geq 0$ and \mathbf{L} is either the identity or a differentiation matrix.¹¹¹ Instead, lasso regression

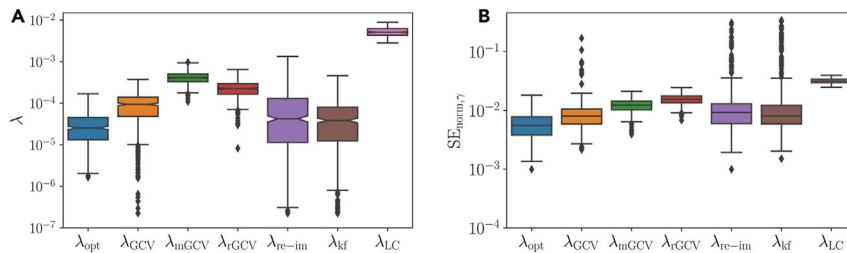


Figure 6. Quantitative comparison of parameter selection methods using artificial EIS measurements

Quantitative comparison of parameter selection methods using artificial EIS spectra; a boxplot of the optimal λ values is presented, alongside those minimizing each cross-validation and L-curve score in (A). The corresponding boxplot of normalized square residuals $SE_{norm,\gamma}$ for each score is displayed in (B). Reproduced with permission from Maradesa et al.³⁸

minimizes the number of zero components in the DRT by choosing $P(\mathbf{x}^*) = \lambda \|\mathbf{x}^*\|_1$ with $\|\mathbf{x}^*\|_1 = \sum_{k=1}^N |x_k^*|$, effectively promoting sparsity.¹⁴ Elastic net regression combines the two ridge and lasso penalties as $P(\mathbf{x}^*) = \lambda_1 \|\mathbf{x}^*\|_1 + \lambda_2 \|\mathbf{L}\mathbf{x}^*\|_2^2$.¹⁰⁴ The regularized regression technique has also been used to study multidimensional EIS spectra.⁹⁶ For impedance spectra exhibiting insufficient resolution at low or high frequencies, an extended log τ domain, defined as $\log \tau_{\min} < \log \tau < \log \tau_{\max}$, can be introduced (τ_{\min} and τ_{\max} are the desired minimum and maximum timescales).¹¹² Importantly, the parameter λ can be obtained optimally using cross-validation,^{38,83,113} data fitting technique,⁸⁸ and other methods.^{39,96} Comparisons of various parameter selection methods are also available as shown in³⁸ (Figure 6). Despite these advantages, limitations persist when analyzing discontinuous DRTs and predicting the DRTs and impedance responses at unprobed frequencies.

To address the challenge of handling discontinuous DRTs, hyperparametric regularized regression has been adopted. Regularization methods can be formulated in a Bayesian context by incorporating prior models, indicating prior experience regarding the EIS data and modeling the DRT as a probability distribution.^{95,101} In this method, a prior model can be also forced on the regularization parameter λ , enabling the detection of DRT discontinuities,⁹⁵ present in the Gerischer, fractal, finite-length Warburg, and piecewise constant elements.¹⁰¹ The weights Ω_{re} and Ω_{im} in (Equation 2) can also be considered as random variables to detect outliers and filter out experimental noise.¹⁰¹ Considering the inherent uncertainties, this approach allows for a more flexible and probabilistic modeling of the DRT.

Fourier transform

Historically, Fourier-transform deconvolution methods were among the first ever used.^{15,94} These methods, directly originating from the early work of Fuoss and Kirkwood,¹¹⁴ stipulates that $\gamma(\log \tau)$ can be obtained by inverse Fourier transforming the imaginary part, $Z_{im}(f)$, of the experimental impedance using the following relation^{15,93,94}:

$$\gamma(\log \tau) = -\frac{4}{\pi} \mathcal{F}^{-1} \left(\frac{\mathcal{F}(Z_{im})(s)}{\operatorname{sech} \left(\frac{\pi}{2} s \right)} \right) (\log \tau) \quad (\text{Equation 3})$$

where \mathcal{F} and \mathcal{F}^{-1} indicate the forward and inverse Fourier transforms, respectively. Despite its simplicity, this method faces limitations in accurately capturing sharp and asymmetric peaks, as well as handling EIS spectra sparsely acquired in frequency. Additionally, it produces noticeable oscillations at the integration range boundaries.⁹⁴ Addressing the presence of errors in experimental spectra necessitates

the application of filtering within the DRT deconvolution process. However, filtering alters the configuration of the DRT peaks.

Genetic algorithms and genetic programming

Genetic algorithms⁸⁶ and genetic programming⁸⁹ have notably been used for DRT deconvolution. Genetic algorithms model the DRT as sums of a finite set of basis functions whose characteristics, such as peak height, position, and spread, are determined through evolutionary algorithms.⁸⁵ This approach focuses on convolution rather than deconvolution. It explores a variety of potential DRT solutions, constituting a solution population, which undergoes evolution driven by evolutionary pressure. Each generation of the population involves the creation, assessment, and merit allocation of new members, based on their response to these evolutionary pressures. The merit, ranging from 0 to 1, influences survival likelihood, with higher values implying greater fitness. Evolutionary pressure encompasses several key factors: (1) overall fitness of the DRT to the EIS data; (2) penalties for complexity (i.e., number of peaks and degrees of freedom), excessively broad peaks, and lack of normalization. The necessity for the normalization penalty can be elucidated as follows: consider a function with N free parameters. The program might fit $N - 1$ of these and determine the N^{th} by ensuring the integral of the DRT across its entire range equals one. However, this method may not be effective, particularly if the chosen normalization factor differs from the actual polarization resistance. Therefore, imposing a normalization constraint as part of evolutionary pressure is a more effective approach.

Impedance spectroscopy by genetic programming (ISGP) is particularly useful when the system has processes that occur in series.⁸⁵ Then, each peak can be linked to specific physical processes, provided timescale separation and a direct physical interpretation is readily available. The area under each peak is the effective resistance, and for the effective capacitance, it is the peak's central time divided by the effective resistance. This is very easy to infer since the peaks are analytical functions. Thanks to the use of analytical functions, it is also reasonably easier to separate partially overlapping processes. Recently, the separation of Faradaic from non-Faradaic contributions to a catalytic material has been demonstrated.^{46,115} Another important advantage of ISGP is the fact that it does not use a filter or regularization parameters, suppressing artifact peaks, as observed in extensive validation on synthetic data. Validation on synthetic experiments has also shown that although the ISGP does not necessarily reconstruct the correct function, it does find the correct number of peaks as well as their positions and areas. Despite the considerable promise, the main disadvantage of the ISGP is the run time, which is in the order of an hour for a single-spectrum EIS data on a regular desktop PC.^{85,89}

Monte Carlo deconvolution

In the context of impedance analysis, Monte-Carlo-based deconvolution^{91,99} has been originally used to study dielectrics. This method minimizes residuals between measured and discretized dielectric constants, which is formally identical to [Equation 2](#), via simulated annealing.⁹¹ Although the Monte Carlo technique offers stability and enables physical parameter evaluation, it demands substantial computational resources, particularly when many sampling steps are required for accurate DRT deconvolution.¹¹⁶

Deep neural networks

Deep neural networks have recently been employed for DRT deconvolution through "one-shot" learning, using either a variation of the deep image prior⁹² or neural

networks approximation of $\gamma(\log \tau)$.¹⁹ In the first instance, the deep prior DRT is a neural network that takes a random variable as input, minimizes Equation 2 by tuning the neural network weights and biases, and outputs the DRT.¹¹⁷ Furthermore, neural networks are universal approximators; therefore, they can be used to approximate the DRT by minimizing a loss function analogous to Equation 2.²⁸ These networks have notable advantages. They are particularly well suited to handle unstructured data.²⁸ Furthermore, despite having many parameters, they can benignly overfit data and can deconvolve the DRT without needing a regularization parameter.^{118,119} Despite its promise, DRT analysis using deep neural networks has some shortcomings, as their training is computationally demanding.

GPs

GPs are an extension of the Bayesian framework that provides a probabilistic approach for regression and classification.^{77,98,120} Gaussian-processes-based deconvolution of the DRT (GP-DRT) assumes the DRT to be a GP, i.e., an infinite set of random variables with any finite subset of these random variables obeying a joint Gaussian distribution. Given that the integral in Equation 1 is a linear functional, the imaginary part of the impedance, $Z_{\text{im}}(f)$, is also a GP.¹²⁰ Therefore, $\gamma(\log \tau)$ can be computed by conditioning the DRT to the experimental impedance as⁸¹

$$\gamma(\log \tau) | Z_{\text{im}}(f) \sim \mathcal{N}(\mu_\gamma, \Sigma_\gamma) \quad (\text{Equation 4})$$

where $Z_{\text{im}}(f)$ is the vector of imaginary parts of the impedance, and μ_γ and Σ_γ represent the DRT mean vector and covariance matrix, respectively. As the measured impedance is assumed to be the sum of model impedance and an error term, the GP kernel yielding Σ_γ is usually optimized to maximize the experimental evidence.^{77,121} The GP-DRT method successfully recovers the DRT, quantifies uncertainty,⁸¹ and predicts the DRT at untested frequencies.^{81,98} However, it uses only the imaginary impedance part and can produce DRTs with negative values. In response to these limitations, the GP-DRT framework has been approximated as a finite GP that utilizes both real and imaginary impedance components and enables the enforcement of the constraint that $\gamma(\log \tau) \geq 0$.^{77,98}

Despite the benefits, GPs suffer from two major drawbacks. First, the computational costs scale cubically with the number of frequencies,⁹⁸ limiting the concurrent analysis of multiple EIS spectra. Second, the evidence maximization prioritizes adherence to experimental data over minimizing the distance between the recovered DRT and the actual DRT.^{81,98} Although conventional GPs are limited by their data-centric nature, structured GPs can incorporate a probabilistic physical model, for example, achieved through analytical expressions and priors on parameter values.¹²² Symbolic regression could also complement structured GPs by searching for the best analytical expression, balancing accuracy with simplicity through genetic programming.¹²³

Combining EIS and time-domain measurements

Recent studies demonstrate the potential of the DRT model to extract impedance from transient voltage responses following a small pulse current.³² Combining this time-domain approach with frequency-resolved EIS can significantly accelerate full-spectra acquisition.³² Faster data collection is crucial for accurate battery impedance measurements, especially at low frequencies where even minor but long excitations can change a battery's state of charge and distort results. Shorter experiment times ensure stationarity for more precise impedance values.⁵⁶ However, it is not possible to assess data quality with a Kramers-Kronig-like test because the underlying model inherently satisfies the Kramers-Kronig relations. This lack of an

established test is a disadvantage compared with EIS. Further research is needed to fully assess the accuracy and resolution of DRT inversion derived from time-domain measurements.

Beyond the DRT

EIS spectra can exhibit resistive-capacitive characteristics¹²⁴ or display resistive-inductive properties. By incorporating an extra kernel, we can express the DRT in an extended or generalized form as follows¹²⁵:

$$Z_{gDRT}(\omega) = Z_{DRT}(\omega) + \int_{-\infty}^{+\infty} \frac{i2\pi f\tau}{1+i2\pi f\tau} h(\log \tau) d \log \tau \quad (\text{Equation 5})$$

where $h(\log \tau)$, an additional DRT-like term,¹²⁶ provides insight into inductive features. The identification of the model parameters requires the solution of an ill-conditioned linear system of equations with a large null space, needing regularization. Furthermore, model (Equation 5) points to the implicit model assumption of a serial connection of elements. Even if the serial connection can be converted into a transmission line model, the topologies that can be represented remain limited.

As explained in the [introduction](#), the DRT is less suitable for analyzing electrochemical systems featuring blocking electrodes.²² The distribution of capacitive times, which models admittance rather than the impedance with a DRT-like model, is emerging as a promising alternative^{127,128} capable of providing insights into the capacitive timescales of the electrochemical systems.¹²⁹ As an alternative approach, the distribution of diffusive times (DDT) model has been used to map EIS data to the diffusional timescales of a distribution of particles or nanowires in batteries or supercapacitors.^{6,130} This allows for linking individual particle models¹³¹ to a radial distribution of particles. The DDT is particularly suitable for modeling diffusive EIS spectra like Warburg-type elements,¹³² but it is limited by the assumption that the electrode is thin.¹³³ This is overcome by the nonlinear DDT model, which extends the DDT to electrodes with finite-thickness.¹³³

For proton-exchange-membrane-based fuel cells and electrolyzers,^{134,135} the low-frequency part of EIS spectra is often influenced by pseudo-inductive features that can be modeled by introducing negative DRT peaks (i.e., within a certain $\log \tau$ range, $\gamma(\log \tau) < 0$).¹³⁶ Considering the Voigt interpretation of the DRT, the interpretation is that an RC element with a negative resistance corresponds to a negative capacitance to ensure timescale positivity (i.e., $\tau = RC > 0$). Although this view on negative DRTs is conceptually appealing, it may compromise interpretability, particularly when the frequencies associated with capacitive and pseudo-inductive processes coincide.¹³⁷

EIS quality assessment

The reliability of DRT analysis is intrinsically associated with the quality of EIS measurements. Widely employed methods for assessing this quality include using Kramers-Kronig relations or the Hilbert transform.¹³⁸ One starts by selecting either the imaginary or real component of the EIS spectrum.^{2,31,139} Subsequently, the Kramers-Kronig relations or Hilbert transform are employed to predict the real or imaginary part of the experimental impedance spectrum. EIS compliance can be assessed by comparing the predicted and measured real or imaginary components using residuals.^{140–142} Recently, methods grounded in Bayesian principles have emerged,¹⁴³ employing sophisticated probability scoring to gauge the “distance” between the probability distribution functions of observed and predicted EIS

spectrum components.^{35,143} It is expected that these advanced quality indices will gain broader adoption, possibly being integrated into software for real-time EIS data assessment.

Hyperparameter optimization

The accuracy of each DRT deconvolution method hinges on hyperparameter selection. Hyperparameters are external configuration variables set before model regression. By contrast, the parameter vector \mathbf{x} defined in [Equation 2](#) is “learned” during regression or training. For example, in ridge regression, λ has a strong influence on the recovered $\gamma(\log \tau)$ as it controls its smoothness and can be optimized using methods like cross-validation^{38,113} among others.³⁹ For neural network inversion, hyperparameters such as the neural network’s width, depth, and architecture can be fine-tuned using a validation set (section [deep neural network](#)).

Furthermore, other parameters, such as the number of iterations used by the optimizer, can be pre-set by employing early stopping as a regularization technique.⁹² In the GP DRT framework, kernel features and error level can be determined by maximizing experimental evidence.^{81,98} In genetic programming, the stopping criterion can be specified as the number of generations where no change occurs in the best solution found.⁸⁵ Other hyperparameters, such as the discretization basis used to approximate $\gamma(\log \tau)$,¹⁷ and the hyperparameters of hyperprior distribution in hyper Bayesian regularized regression^{95,101} can be determined using grid/random search.^{144,145} Likewise, in genetic algorithms, crossover and mutation rates (section [genetic algorithms and genetic programming](#)), the number of Monte Carlo steps (section [monte carlo deconvolution](#)),⁹⁹ and the window width for the inverse Fourier transform⁹³ can be statistically optimized through cross-validation,³⁸ and Akaike/Bayesian information criteria,¹⁴⁶ although this aspect remains largely unexplored.

FUTURE DIRECTIONS FOR METHOD DEVELOPMENT

The earlier sections of this paper emphasized the importance of the DRT method in analyzing EIS data, highlighted existing challenges, and identified user requirements for future development (based on survey data). This section outlines strategies to augment DRT methods, focusing on establishing impedance databases, creating standardized benchmarks, developing automated DRT deconvolution processes, and enhancing software capabilities to facilitate wider utilization.

Challenges and opportunities

In the current age of prolific data generation, there is vast and continuous data generation. Yet, considerable challenges exist in effectively collecting high-quality data and accurately analyzing them. For example, combinatorial synthesis of materials expedites the study of material-structure relationships, a critical aspect of material research.^{67,147} This acceleration is also observed in the development of battery assembly and discovery using robotic systems.¹⁴⁸ However, data analysis often faces bottlenecks, such as the time-consuming acquisition of EIS measurements. Accelerated time-dependent conventional impedance methods³² and multi-frequency analysis¹⁴⁹ offer a solution to this issue by substantially reducing acquisition times.³² Analyzing large EIS datasets requires an advanced, coherent framework capable of multidimensional analysis ([Figure 3](#)). The utilization of machine-learning-assisted equivalent circuit identification could potentially resolve the aforementioned issue.^{150,151} However, as the complexity of the circuits increases, the task of identifying optimal parameters during the regression process becomes increasingly complicated. Moreover, the development of a single universally applicable equivalent circuit is difficult. The DRT provides a flexible, coherent, and non-parametric

alternative to these conventional model-based methods. For instance, it allows for the recovery across timescales in a unified setting and offers a unique visual interpretation, which is unattainable by analyzing EIS spectra or circuits alone.

Developing large-scale EIS-based repositories comprising synthetic and curated experimental EIS spectra could be highly beneficial to the field.¹⁵² On the one hand, the database of synthetic data could be used to systematically benchmark methods against standard ones. On the other hand, curated EIS spectra comprising equivalent circuits and ancillary experimental data could inform the creation of time-scale peak databases, a blueprint akin to an “impedance genome.” In principle, advanced DRT software could perform multidimensional fitting, peak association, and interpretation, heralding a new, efficient approach to impedance analysis, aiding interpretability, and allowing quantitative assignment of the DRT features to physical processes.

It is apparent from the discussion above that the deconvolution methods described in section [DRT-based deconvolution and analysis methods](#) remain pivotal to advancing the DRT field. Neural networks are particularly powerful because, as explained above, they can easily handle unstructured data and multidimensional fitting without suffering from the curse of dimensionality.²⁸ These neural networks can be used for one-shot regression with regularization or as inversion machines. In both cases, regularized regression or other methods can supplement or pretrain the model. For instance, pre-training^{19,119} or pre-inversion offers potential benefits to speed up neural network optimization or to improve deconvolution accuracy.^{19,28}

Probabilistic strategies such as Bayesian DRT methods^{18,101} and GP^{81,98} also merit consideration due to their capability to quantify uncertainty and robustness to experimental noise. In data quality assessment, the role of GPs and other probabilistic scoring approaches cannot be overlooked. To accelerate EIS acquisition, the experimentalists can employ optimal experimental design, which offers statistically oriented techniques for selecting the next optimal experimental data.^{153,154} Utilizing optimal experimental design can enhance parameter estimation accuracy and substantially reduce experimental time.¹⁵⁵ Incorporating the Kramers-Kronig transform and advanced probabilistic scoring into DRT software is essential.

These observations also point to the development of a complete and automated DRT framework to enhance confidence in the quality of DRT inversion and, consequently, the adoption of DRT methods in other research fields. The current integration of DRT methods with software platforms remains limited, sometimes involving the repurposing of existing software. Overall, the DRT community should prioritize developing sophisticated frameworks to broaden DRT applications across various disciplines and to promote interdisciplinary synergies.

Advancing DRT usage and future pathways

Given insights derived from the survey (section [survey](#)) and the limitations of the existing deconvolution techniques (section [DRT-based deconvolution and analysis methods](#)), expanding DRT methods is imperative. As emphasized in section [DRT workflow and applications](#), automating DRT deconvolution is crucial to offering seamless DRT analysis, minimizing human error, and improving the reliability of results. To fully automate the deconvolution process illustrated in [Figure 2](#), it is necessary to streamline implementations, including the following tasks: (1) data upload; (2) quality assessment of EIS data to facilitate data curation, including model systems experimental error evaluation; (3) DRT deconvolution with minimal input from users;

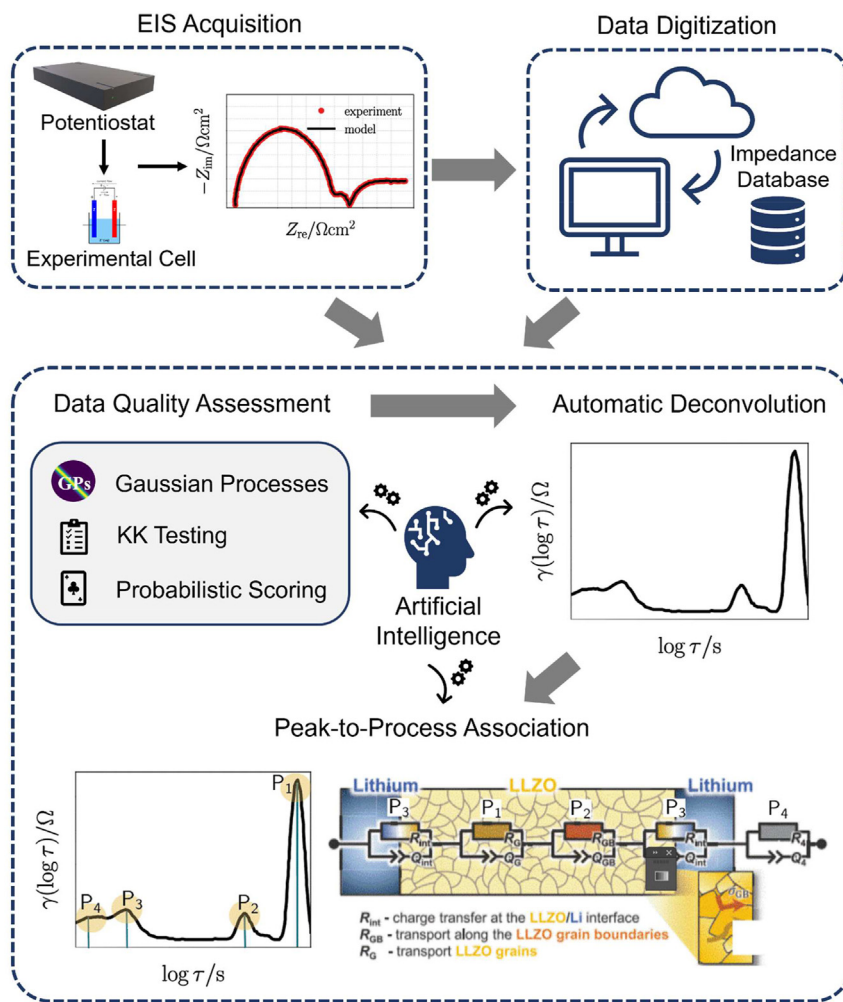


Figure 7. AI-based automation of the entire deconvolution process

Reproduced with permission from Müller et al.⁴¹

and (4) association of peaks or peak patterns to specific processes (Figure 7). Most of these functionalities are currently absent in existing DRT software; however, software equipped with these advanced features possesses the potential to greatly influence the field. The DRT characteristic obtained through these features can be additionally aggregated, resulting in an automated regularization.¹⁶ Furthermore, integrating these sophisticated DRT frameworks into experimental configurations offers a promising opportunity for real-time quality evaluation and DRT deconvolution concurrently with data collection. By establishing a direct link between software and experiments, researchers could promptly derive insights into the impact of experimental conditions on the DRT deconvolution,⁸⁰ guiding subsequent experiments and enhancing research productivity.

As detailed in section [survey](#), there is a significant need for the automation of DRT deconvolution and peak assignment, along with the batch processing of EIS data. This underscores the critical need for a more widespread adoption of AI-based methods in the DRT field. Survey respondents suggested that DRT software should incorporate advanced features such as peak-to-process association and automatic timescale separation, which would improve the interpretability of DRT results.

Integrating Bayesian statistics into the DRT framework enables the calculation of peak occurrence probabilities and automatic distinction between real and pseudo peaks, thus yielding more accurate and insightful analysis.^{18,101,156} In the battery sector, there is also interest in employing the DRT to tackle non-convergence in EIS (i.e., EIS data exhibiting behavior related to mass-transport processes) and to quantify impedance related to specific electrochemical processes. The DRT is limited in its capability to accurately study non-convergent EIS. Although an alternative, the distribution of capacitive times, exists, it remains largely unexplored.^{129,157} Although DRT is useful in process identification, precise impedance quantification frequently requires simulation, which can be less efficient. Therefore, developments enabling DRT methods to substitute for simulations are highly promising.

Documenting the quality of DRT methods implementations

Validating and establishing benchmarks for DRT methods is crucial for verifying their performance and gaining trust, especially in automated verification scenarios. In contrast to machine-learning fields such as computer vision, natural language processing, and reinforcement learning, where standardized testing is a common practice,¹⁵⁸ the DRT field does not yet have such established practices and databases. To bridge this gap, it is essential to develop standardized software testing procedures and establish criteria for certifying the effectiveness of new DRT methods or software. In that context, a collaborative effort should be made to create standardized libraries of both artificial and real impedance datasets to facilitate the validation of new methods. Secondly, advanced methods rooted in statistics should be introduced for robust validation. For example, in the field of vision¹⁵⁹ and natural language processing,¹⁶⁰ researchers rely on existing databases to assess algorithms. Similarly, the DRT community could establish a benchmark impedance database to test and validate new methods and software. Furthermore, having as a community effort in which software is shared and benchmarked would result in increased output quality.

Advancing DRT software

Standardization of DRT methods and software

Similar to how PyTorch¹⁶¹ has become the lingua franca in the deep-learning field, thereby streamlining model development, DRT can benefit from a unified software paradigm. As seen in the machine-learning field, interoperability would be enhanced, gold standards for the field would be established, and if properly documented, new entrants would have an easier time. The standardization of DRT software may inspire governments and other public sectors to actively support the field to foster progress and innovation. Ultimately, undertaking these tasks would propel the field's advancement and further encourage DRT adoption beyond current use. For instance, researchers in other fields, such as biology, sensors, corrosion, and electro- and photocatalysis, may be more prone to use these methods if their reliability and usefulness are proven. To this end, adopting standardized procedures for code performance, readability, and user-friendliness is essential.

Open-source strategies and community collaboration for EIS research

Insights from the survey data presented in section [Survey](#) underscore the role of open-source software in promoting accessibility and transparency, which are critical for driving innovations through joint efforts.³⁶ The integration of open-source philosophies in the development of DRT software yields significant benefits by fostering communal knowledge, expediting research, and incorporating a variety of perspectives, which are advantageous to the EIS community. Establishing standardized protocols encourages collaboration and accelerates advancements, much like the

success seen in the machine-learning community.¹⁶² The open-source deployment of DRT software would attract proficient researchers, further promoting the quality and depth of DRT-based research, thus expediting material discovery. Open-source strategies create a collective repository of knowledge, particularly instrumental in promoting the growth of the DRT field. In addition, the adoption of standardized practices, open-source deployment of DRT software, and the creation of large impedance databases could catalyze the creation of a collaborative ecosystem, thus expanding the talent pool and accelerating the dissemination of scientific knowledge.

Existing free and open-source DRT software. A wide range of free and open-source DRT software packages are available, many with graphical user interfaces (GUIs). These include DRTtools,^{17,163} pyDRTtools,^{17,164} DRT-RBLM,^{40,165} DearEIS,¹⁶⁶ ED-DRT,¹¹² LEVM/LEVMW,¹⁶⁷ and ISGP,⁸⁵ as well as others^{18,19,28,81,88,92,98,110,168} (see Table S10 in Ciucci et al.⁸⁰ for additional commercial software). These packages were developed using the deconvolution methods described in section **DRT deconvolution**. While powerful, existing tools cannot fully automate DRT deconvolution and reliably correlate peaks with specific processes (Figure 7). Collaborative, scientific-community-driven efforts to automate the deconvolution steps described in section **advancing DRT usage and future pathways** hold the promise of significantly simplifying DRT analysis, thus making it accessible to a wider range of researchers.

CONCLUSIONS

EIS has proven to be a powerful diagnostic technique for the characterization of electrochemical systems across various fields. Despite several limitations, the DRT represents a promising non-parametric approach for analyzing EIS data. This article outlines the key concepts related to this distribution function and highlights several critical areas for future research to enrich the applicability of this technique, as informed by survey findings. To this end, a crucial step involves standardizing DRT methods and software, fully automating deconvolution, and creating benchmark tools for validation. These practices aim to facilitate a unified DRT software ecosystem developed collaboratively to bring substantial advancement to the EIS community. Additionally, this article is expected to facilitate innovative and advanced DRT-based research in electrochemical systems through a research roadmap tailored to the needs of the researchers who rely on DRT analysis to expedite material discovery and optimize system performance. It is anticipated that DRT will foster a broader spectrum of research applications, extending beyond electrochemistry into various other fields of knowledge, such as medicine, bioengineering, etc., and consequently, accelerating research discovery.

DATA AVAILABILITY

Data and supplementary materials are available at <https://github.com/ciuccislab/DRT-Survey>.⁸⁰

ACKNOWLEDGMENTS

A.M., B.P., and F.C. gratefully acknowledge the Research Grant Council of Hong Kong for support through projects 18201820 and 16201622. A.M. and B.P. kindly thank the Hong Kong PhD Fellowship Scheme for its financial support. F.C. thanks the University of Bayreuth and the Bavarian Center for Battery Technology (BayBatt) for providing a start-up fund. R.O. and J.H. acknowledge support from the Hydrogen in Energy and Information Sciences (HEISs) center, an Energy Frontier Research Center funded by the U.S. Department of Energy (DOE), Office of Science, Basic Energy

Sciences (BES), under award no. DE-SC0023450 (DRT estimation methodology and software development), and by the Army Research Office (ARO) under Award 1305 no. W911NF-22-1-0273 (experimental application of EIS/DRT to electrochemical devices), and as part of the Energy Frontier Research Centers program: CSSAS-The Center for the Science of Synthesis Across Scales under award no. DE-SC0019288.

AUTHOR CONTRIBUTIONS

A.M.: survey design, data collection, data curation, formal analysis, visualization, writing – review & editing, writing – original draft. B.P.: visualization, writing – review & editing. J.H.: visualization, writing – review & editing. Y.L.: writing – review & editing. P.I.: writing – review & editing. A.M.: writing – review & editing. H.M.L.: visualization, writing – review & editing. Y.W.: data collection, writing – review & editing. Z.W.: writing – review & editing. J. Li: writing – review & editing. S.X.: writing – review & editing. Q.M.: writing – review & editing. J. Liu: writing – review & editing. C.B.: supervision, writing – review & editing. A.G.: writing – review & editing. K.K.: writing – review & editing. A.B.: writing – review & editing. N.J.W.: writing – review & editing. C.Z.: supervision, writing – review & editing. M.D.: writing – review & editing. M.Z.: writing – review & editing. P.W.: writing – review & editing. V.Y.: writing – review & editing. S.P.: writing – review & editing. Y.C.: writing – review & editing. A.W.: writing – review & editing. S.V.K.: funding acquisition, writing – review & editing. J.P.S.: writing – review & editing. Y.T.: writing – review & editing. B.A.B.: writing – review & editing. Q.Z.: supervision, writing – review & editing. M.G.: writing – review & editing. R.O.: supervision, visualization, funding acquisition, writing – review & editing. F.C.: survey design, data collection, resources, project administration, funding acquisition, supervision, writing – review & editing, writing – original draft.

DECLARATION OF INTERESTS

The authors declare no competing interests.

DECLARATION OF GENERATIVE AI AND AI-ASSISTED TECHNOLOGIES IN THE WRITING PROCESS

Upon editing the manuscript, the authors used Gemini Advanced to improve readability. After using this tool, the authors reviewed and re-edited the content as needed. The authors take full responsibility for the content of the published article.

REFERENCES

1. Vivier, V., and Orazem, M.E. (2022). Impedance analysis of electrochemical systems. *Chem. Rev.* 122, 11131–11168. <https://doi.org/10.1021/acs.chemrev.1c00876>.
2. Wang, S., Zhang, J., Gharbi, O., Vivier, V., Gao, M., and Orazem, M.E. (2021). Electrochemical impedance spectroscopy. *Nat. Rev. Methods Primers* 1, 41. <https://doi.org/10.1038/s43586-021-00039-w>.
3. Sadeghi, E., Gholami, M.M., Hamzeh, M., Alavi, S.M.M., and Saif, M. (2023). A systematic overview of power electronics interfaced electrochemical impedance spectroscopy for energy storage systems. *J. Energy Storage* 62, 106850. <https://doi.org/10.1016/j.est.2023.106850>.
4. Sanginario, A., and Hernández, S. (2023). Diagnostics of electrocatalytic systems by electrochemical impedance spectroscopy. *Curr. Opin. Green Sustain. Chem.* 39, 100727. <https://doi.org/10.1016/j.cogsc.2022.100727>.
5. Fariati, G.C., Duongt, D.T., Salleo, A., Polyzoidis, C.A., Logothetidis, S., Rivnay, J., Owens, R., and Malliaras, G.G. (2014). Organic electrochemical transistors as impedance biosensors. *MRS Commun.* 4, 189–194. <https://doi.org/10.1557/mrc.2014.35>.
6. Ciucci, F. (2019). Modeling electrochemical impedance spectroscopy. *Curr. Opin. Electrochem.* 13, 132–139. <https://doi.org/10.1016/j.coelec.2018.12.003>.
7. Schönleber, M., and Ivers-Tiffée, E. (2015). Approximability of impedance spectra by RC elements and implications for impedance analysis. *Electrochim. Commun.* 58, 15–19. <https://doi.org/10.1016/j.elecom.2015.05.018>.
8. Macdonald, D.D. (2006). Reflections on the history of electrochemical impedance spectroscopy. *Electrochim. Acta* 51, 1376–1388. <https://doi.org/10.1016/j.electacta.2005.02.107>.
9. Zhu, H., and Kee, R.J. (2006). Modeling electrochemical impedance spectra in SOFC Button cells with internal methane reforming. *J. Electrochem. Soc.* 153, A1765–A1772. <https://doi.org/10.1149/1.2220065>.
10. Lu, Y., Zhao, C.Z., Huang, J.Q., and Zhang, Q. (2022). The timescale identification decoupling complicated kinetic processes in lithium batteries. *Joule* 6, 1172–1198. <https://doi.org/10.1016/j.joule.2022.05.005>.
11. Kobayashi, K., and Suzuki, T.S. (2022). Extended distribution of relaxation times analysis for electrochemical impedance spectroscopy. *Electrochemistry* 90, 017004.

12. The DRT impedance model in (Equation 1) is quite standard; some other variants can be found in the literature^{6,11,18}.
13. We stress that $\gamma(\log \tau) = \tau g(\tau)$, with $g(\tau)$ denoting a non-negative timescale distribution; further details can be found elsewhere^{6,14}.
14. Saccoccio, M., Wan, T.H., Chen, C., and Ciucci, F. (2014). Optimal regularization in distribution of relaxation times applied to electrochemical impedance spectroscopy: Ridge and lasso regression methods - a theoretical and experimental study. *Electrochim. Acta* 147, 470–482. <https://doi.org/10.1016/j.electacta.2014.09.058>.
15. Schichlein, H., Müller, A.C., Voigts, M., Krugal, A., and Ivers-Tiffée, E. (2002). Deconvolution of electrochemical impedance spectra for the identification of electrode reaction mechanisms in solid oxide fuel cells. *J. Appl. Electrochem.* 32, 875–882.
16. Žic, M., Pereverzyev, S.V., Subotić, V., and Pereverzyev, S. (2020). Adaptive multi-parameter regularization approach to construct the distribution function of relaxation times. *Int. J. Geomath.* 11, 2. <https://doi.org/10.1007/s13137-019-0138-2>.
17. Wan, T.H., Saccoccio, M., Chen, C., and Ciucci, F. (2015). Influence of the discretization methods on the distribution of relaxation times deconvolution: Implementing radial basis functions with DRTtools. *Electrochim. Acta* 184, 483–499. <https://doi.org/10.1016/j.electacta.2015.09.097>.
18. Huang, J., Papac, M., and O'Hare, R. (2021). Towards robust autonomous impedance spectroscopy analysis: A calibrated hierarchical Bayesian approach for electrochemical impedance spectroscopy (EIS) inversion. *Electrochim. Acta* 367, 137493. <https://doi.org/10.1016/j.electacta.2020.137493>.
19. Quattrochi, E., Py, B., Maradesa, A., Meyer, Q., Zhao, C., and Ciucci, F. (2023). Deconvolution of electrochemical impedance spectroscopy data using the deep-neural-network-enhanced distribution of relaxation times. *Electrochim. Acta* 439, 141499. <https://doi.org/10.1016/j.electacta.2022.141499>.
20. Ivers-Tiffée, E., and Webér, A. (2017). Evaluation of electrochemical impedance spectra by the distribution of relaxation times. *J. Ceram. Soc. Japan* 125, 193–201. <https://doi.org/10.2109/jcersj2.16267>.
21. Illig, J., Ender, M., Chrobak, T., Schmidt, J.P., Klotz, D., and Ivers-Tiffée, E. (2012). Separation of charge transfer and contact resistance in LiFePO₄-cathodes by impedance modeling. *J. Electrochem. Soc.* 159, A952.
22. Lu, Y., Zhao, C.Z., Hu, J.K., Sun, S., Yuan, H., Fu, Z.H., Chen, X., Huang, J.Q., Ouyang, M., and Zhang, Q. (2022). The void formation behaviors in working solid-state Li metal batteries. *Sci. Adv.* 45, eadd0510.
23. Sun, S., Zhao, C., Yuan, H., Fu, Z.H., Chen, X., Lu, Y., Li, Y., Hu, J., Dong, J., Huang, J., et al. (2022). Eliminating interfacial O-involving degradation in Li-Rich Mn-based cathodes for all-solid-state lithium batteries. *Sci. Adv.* 8, eadd5189.
24. Dierickx, S., Webér, A., and Ivers-Tiffée, E. (2020). How the distribution of relaxation times enhances complex equivalent circuit models for fuel cells. *Electrochim. Acta* 355, 136764. <https://doi.org/10.1016/j.electacta.2020.136764>.
25. Douglan, J.C., Vijaya Sankar, K.V., Biancolli, A.L.G., Santiago, E.I., Tsur, Y., and Dekel, D.R. (2023). Quantifying the resistive losses of the catalytic layers in anion-exchange membrane fuel cells. *ChemSusChem* 16, e202301080. <https://doi.org/10.1002/cssc.202301080>.
26. Oz, A., Herskowitz, S., Belman, N., Tal-Gutelmacher, E., and Tsur, Y. (2016). Analysis of impedance spectroscopy of aqueous supercapacitors by evolutionary programming: Finding DFRT from complex capacitance. *Solid State Ionics* 288, 311–314. <https://doi.org/10.1016/j.ssi.2015.11.008>.
27. Van Haeverbeke, M., De Baets, B., and Stock, M. (2023). Evaluating the potential of distribution of relaxation times analysis for plant agriculture. *Comput. Electron. Agric.* 213, 108249. <https://doi.org/10.1016/j.compag.2023.108249>.
28. Quattrocchi, E., Wan, T.H., Belotti, A., Kim, D., Pepe, S., Kalinin, S.V., Ahmadi, M., and Ciucci, F. (2021). The deep-DRT: A deep neural network approach to deconvolve the distribution of relaxation times from multidimensional electrochemical impedance spectroscopy data. *Electrochim. Acta* 392, 139010. <https://doi.org/10.1016/j.electacta.2021.139010>.
29. Leonide, A., Sonn, V., Webér, A., and Ivers-Tiffée, E. (2008). Evaluation and modeling of the cell resistance in anode-supported solid oxide fuel cells. *J. Electrochem. Soc.* 155, B36. <https://doi.org/10.1149/1.2801372>.
30. Hori, S., Kanno, R., Sun, X., Song, S., Hirayama, M., Hauck, B., Dippon, M., Dierickx, S., and Ivers-Tiffée, E. (2023). Understanding the impedance spectra of all-solid-state lithium battery cells with sulfide superionic conductors. *J. Power Sources* 556, 232450. <https://doi.org/10.1016/j.jpowsour.2022.232450>.
31. Boukamp, B.A. (1995). A linear Kronig-Kramers transform test for immittance data validation. *J. Electrochim. Soc.* 142, 1885–1894. <https://doi.org/10.1149/1.2044210>.
32. Schmidt, J.P., and Ivers-Tiffée, E. (2016). Pulse-Fitting – A novel method for the evaluation of pulse measurements, demonstrated for the low frequency behavior of lithium-ion cells. *J. Power Sources* 315, 316–323. <https://doi.org/10.1016/j.jpowsour.2016.03.026>.
33. While the process of solving the integral Equation 1 is often called “DRT deconvolution,” the underlying integral differs from the signal processing definition of convolution and its inverse, the deconvolution.
34. Iurilli, P., Brivio, C., Carrillo, R.E., and Wood, V. (2022). Physics-based SoH estimation for Li-Ion Cells. *Batteries* 8, 204. <https://doi.org/10.3390/batteries8110204>.
35. Ciucci, F. (2020). The Gaussian process Hilbert transform (GP-HT): Testing the consistency of electrochemical impedance spectroscopy data. *J. Electrochim. Soc.* 167, 126503. <https://doi.org/10.1149/1945-7111/aba937>.
36. Di Tommaso, P.D., Chatzou, M., Floden, E.W., Barja, P.P., Palumbo, E., and Notredame, C. (2017). Nextflow enables reproducible computational workflows. *Nat. Biotechnol.* 35, 316–319. <https://doi.org/10.1038/nbt.3820>.
37. Huang, J., Sullivan, N.P., Zakutayev, A., and O’Hayre, R. (2023). How Reliable Is distribution of relaxation times (DRT) Analysis? a dual regression-classification perspective on DRT estimation, interpretation, and accuracy. *Electrochim. Acta* 443, 141879. <https://doi.org/10.1016/j.electacta.2023.141879>.
38. Maradesa, A., Py, B., Wan, T.H., Effat, M.B., and Ciucci, F. (2023). Selecting the regularization parameter in the distribution of relaxation times. *J. Electrochim. Soc.* 170, 030502. <https://doi.org/10.1149/1945-7111/acbca4>.
39. Hansen, P.C., and O’Leary, D.P. (1993). The use of the L-curve in the regularization of discrete ill-posed problems. *SIAM J. Sci. Comput.* 14, 1487–1503. <https://doi.org/10.1137/0914086>.
40. Kunaver, M., Rojec, Ž., Subotić, V., Pereverzyev, S., and Žic, M. (2022). Extraction of distribution function of relaxation times by using DRT-RBLM tools: A new approach to combine Levenberg-Marquardt algorithm and radial basis functions for discretization basis. *J. Electrochim. Soc.* 169, 110529. <https://doi.org/10.1149/1945-7111/ac9a83>.
41. Müller, M., Schmieg, J., Dierickx, S., Joos, J., Webér, A., Gerthsen, D., and Ivers-Tiffée, E. (2022). Reducing impedance at a Li-metal anode/garnet-type electrolyte interface implementing chemically resolvable in layers. *ACS Appl. Mater. Interfaces* 14, 14739–14752. <https://doi.org/10.1021/acsami.1c25257>.
42. Zheng, Y., Shi, Z., Guo, D., Dai, H., and Han, X. (2021). A Simplification of the time-domain equivalent circuit model for lithium-ion batteries based on low-frequency electrochemical impedance spectra. *J. Power Sources* 489, 229505. <https://doi.org/10.1016/j.jpowsour.2021.229505>.
43. Meddings, N., Heinrich, M., Overney, F., Lee, J.-S., Ruiz, V., Napolitano, E., Seitz, S., Hinds, G., Racchichini, R., Gaberšček, M., et al. (2020). Application of electrochemical impedance spectroscopy to commercial Li-ion cells: A review. *J. Power Sources* 480, 228742. <https://doi.org/10.1016/j.jpowsour.2020.228742>.
44. Schmidt, J.P., Chrobak, T., Ender, M., Illig, J., Klotz, D., and Ivers-Tiffée, E. (2011). Studies on LiFePO₄ as cathode material using impedance spectroscopy. *J. Power Sources* 196, 5342–5348. <https://doi.org/10.1016/j.jpowsour.2010.09.121>.
45. Yan, C., Jiang, L.-L., Yao, Y.-X., Lu, Y., Huang, J.-Q., and Zhang, Q. (2021). Nucleation and growth mechanism of anion-derived solid electrolyte interphase in rechargeable batteries. *Angew. Chem. Int. Ed. Engl.* 60,

- 8521–8525. <https://doi.org/10.1002/anie.202100494>.
46. Attias, R., Bhowmick, S., and Tsur, Y. (2023). Distribution function of relaxation times: an alternative to classical methods for evaluating the reaction kinetics of oxygen evolution reaction. *Chem. Eng. J.* 476, 146708. <https://doi.org/10.1016/j.cej.2023.146708>.
47. Steinhauer, M., Risso, S., Wagner, N., and Friedrich, K.A. (2017). Investigation of the solid electrolyte interphase formation at graphite anodes in lithium-ion batteries with electrochemical impedance spectroscopy. *Electrochim. Acta* 228, 652–658. <https://doi.org/10.1016/j.electacta.2017.01.128>.
48. Uhlmann, C., Braun, P., Illig, J., Webér, A., and Ivers-Tiffée, E. (2016). Interface and grain boundary resistance of a lithium lanthanum titanate ($\text{Li}_{3x}\text{La}_{2/3-x}\text{TiO}_3$, LLTO) solid electrolyte. *J. Power Sources* 307, 578–586. <https://doi.org/10.1016/j.jpowsour.2016.01.002>.
49. Chen, H., Zhang, H., Zhou, Y., Chen, J., Huang, X., and Tian, B. (2023). Structure-conduction correlations in a chlorine-rich superionic lithium-argyrodite solid electrolyte: a DRT Analysis. *J. Power Sources* 583, 233579. <https://doi.org/10.1016/j.jpowsour.2023.233579>.
50. Presci, F.M., Bertei, A., Brugge, R.H., Emge, S.P., Hekelman, A.K.O., Marbella, L.E., Grey, C.P., and Aguadero, A. (2020). Establishing ultralow activation energies for lithium transport in garnet electrolytes. *ACS Appl. Mater. Interfaces* 29, 32806–32816.
51. Paul, T., Yavo, N., Lubomirsky, I., and Tsur, Y. (2019). Determination of grain boundary conductivity using distribution function of relaxation times (DFRT) analysis at room temperature in 10 mol% Gd doped ceria: A non-classical electrostrictor. *Solid State Ionics* 331, 18–21. <https://doi.org/10.1016/j.ssi.2018.12.013>.
52. Risso, S., Härk, E., Kent, B., and Ballauff, M. (2019). Operando analysis of a lithium/sulfur battery by small-angle neutron scattering. *ACS Nano* 13, 10233–10241. <https://doi.org/10.1021/acsnano.9b03453>.
53. Su, Y.-H., Chung, C.-Y., Chen, Y.-R., Wu, F.-Y., Lin, Y.-H., Chi, P.-W., Wu, P.M., Paul, T., Lin, H.-E., Chang-Liao, K.-S., et al. (2023). A green recyclable Li_3VO_4 -pectin electrode exhibiting pseudocapacitive effect as an advanced anode for lithium-ion battery. *J. Energy Storage* B 72, 108454. <https://doi.org/10.1016/j.est.2023.108454>.
54. Lu, Y., Zhao, C.-Z., Zhang, R., Yuan, H., Hou, L.-P., Fu, Z.-H., Chen, X., Huang, J.-Q., and Zhang, Q. (2021). The carrier transition from Li atoms to Li vacancies in solid-state lithium alloy anodes. *Sci. Adv.* 7, eabi5520. <https://doi.org/10.1126/sciadv.abi5520>.
55. Wang, J., Zhao, R., Huang, Q.-A., Wang, J., Fu, Y., Li, W., Bai, Y., Zhao, Y., Li, X., and Zhang, J. (2023). High-efficient prediction of state of health for lithium-ion battery based on AC impedance feature tuned with Gaussian process regression. *J. Power Sources* 561, 232737. <https://doi.org/10.1016/j.jpowsour.2023.232737>.
56. Wildfeuer, L., Wassiliadis, N., Karger, A., Bauer, F., and Lienkamp, M. (2022). Teardown analysis and characterization of a commercial lithium-ion battery for advanced algorithms in battery electric vehicles. *J. Energy Storage* 48, 103909. <https://doi.org/10.1016/j.est.2021.103909>.
57. Lai, X., Huang, Y., Gu, H., Deng, C., Han, X., Feng, X., and Zheng, Y. (2021). Turning waste into wealth: A systematic review on echelon utilization and material recycling of retired lithium-ion batteries. *Energy Storage Mater.* 40, 96–123. <https://doi.org/10.1016/j.ensm.2021.05.010>.
58. He, R., He, Y., Xie, W., Guo, B., and Yang, S. (2023). Comparative analysis for commercial Li-ion batteries degradation using the distribution of relaxation time method based on electrochemical impedance spectroscopy. *Energy* 263, 125972. <https://doi.org/10.1016/j.energy.2022.125972>.
59. Lyu, Z., Li, H., Han, M., Sun, Z., and Sun, K. (2022). Performance degradation analysis of solid oxide fuel cells using dynamic electrochemical impedance spectroscopy. *J. Power Sources* 538, 231569. <https://doi.org/10.1016/j.jpowsour.2022.231569>.
60. Liu, S., Meyer, Q., Jia, C., Wang, S., Rong, C., Nie, Y., and Zhao, C. (2023). Operando Deconvolution of the degradation mechanisms of iron–nitrogen–carbon catalysts in proton exchange membrane fuel cells. *Energy Environ. Sci.* 16, 3792–3802. <https://doi.org/10.1039/D3EE01166F>.
61. Heinzmüller, M., Webér, A., and Ivers-Tiffée, E. (2018). Advanced impedance study of polymer electrolyte membrane single cells by means of distribution of relaxation times. *J. Power Sources* 402, 24–33. <https://doi.org/10.1016/j.jpowsour.2018.09.004>.
62. Drach, Z., Hershkovitz, S., Ferrero, D., Leone, P., Lanzini, A., Santarelli, M., and Tsur, Y. (2016). Impedance spectroscopy analysis inspired by evolutionary programming as a diagnostic tool for SOEC and SOFC. *Solid State Ionics* 288, 307–310. <https://doi.org/10.1016/j.ssi.2016.01.001>.
63. Endler, C., Leonide, A., Webér, A., Tietz, F., and Ivers-Tiffée, E. (2010). Time-dependent electrode performance changes in intermediate temperature solid oxide fuel cells. *J. Electrochem. Soc.* 157, B292. <https://doi.org/10.1149/1.3270047>.
64. Müller-Hülsede, J., Schmies, H., Schonvogel, D., Meyer, Q., Nie, Y., Zhao, C., Wagner, P., and Wark, M. (2024). What determines the stability of Fe–N–C catalysts in HT-PEMFCs? *Intl. J. Hydrog. Energy* 50, 921–930. <https://doi.org/10.1016/j.ijhydene.2023.09.190>.
65. Müller-Hülsede, J., Zierdt, T., Schmies, H., Schonvogel, D., Meyer, Q., Zhao, C., Wagner, P., and Wark, M. (2022). Implementation of different Fe–N–C catalysts in high temperature proton exchange membrane fuel cells – effect of catalyst and catalyst layer on performance. *J. Power Sources* 537, 231529. <https://doi.org/10.1016/j.jpowsour.2022.231529>.
66. Meyer, Q., Liu, S., Li, Y., and Zhao, C. (2022). Operando detection of oxygen reduction reaction kinetics of Fe–N–C catalysts in proton exchange membrane fuel cells. *J. Power Sources* 533, 231058. <https://doi.org/10.1016/j.jpowsour.2022.231058>.
67. Gregoire, J.M., Zhou, L., and Haber, J.A. (2023). Combinatorial synthesis for AI-driven materials discovery. *Nat. Synth.* 2, 493–504. <https://doi.org/10.1038/s44160-023-00251-4>.
68. Dastafkan, K., Shen, X., Hocking, R.K., Meyer, Q., and Zhao, C. (2023). Monometallic Interphasic synergy via nano-hetero-interfacing for hydrogen evolution in alkaline electrolytes. *Nat. Commun.* 14, 547. <https://doi.org/10.1038/s41467-023-36100-3>.
69. Jia, C., Zhao, Y., Song, S., Sun, Q., Meyer, Q., Liu, S., Shen, Y., and Zhao, C. (2023). Highly ordered hierarchical porous single-atom Fe catalyst with promoted mass transfer for efficient electroreduction of CO_2 . *Adv. Energy Mater.* 13, 2302007. <https://doi.org/10.1002/aenm.202302007>.
70. Wang, Q., Hu, Z., Xu, L., Li, J., Gan, Q., Du, X., and Ouyang, M. (2021). A comparative study of equivalent circuit model and distribution of relaxation times for fuel cell impedance diagnosis. *Int. J. Energy Res.* 45, 15948–15961. <https://doi.org/10.1002/er.6825>.
71. Xia, J., Wang, C., Wang, X., Bi, L., and Zhang, Y. (2020). A perspective on DRT applications for the analysis of solid oxide cell electrodes. *Electrochim. Acta* 349, 136328. <https://doi.org/10.1016/j.electacta.2020.136328>.
72. Mroziński, A., Molin, S., Karczewski, J., Miruszewski, T., and Jasinski, P. (2019). Electrochemical properties of porous $\text{Sr}_{0.86}\text{Ti}_{0.45}\text{Fe}_{0.35}\text{O}_3$ oxygen electrodes in solid oxide cells: Impedance study of symmetrical electrodes. *Intl. J. Hydrog. Energy* 44, 1827–1838. <https://doi.org/10.1016/j.ijhydene.2018.11.203>.
73. Shi, N., Su, F., Huan, D., Xie, Y., Lin, J., Tan, W., Peng, R., Xia, C., Chen, C., and Lu, Y. (2017). Performance and DRT analysis of P-SOFCs fabricated using new phase inversion combined tape casting technology. *J. Mater. Chem. A* 5, 19664–19671. <https://doi.org/10.1039/C7TA04967F>.
74. Lyagaeva, J., Vdovin, G., Hakimova, L., Medvedev, D., Demin, A., and Tsikararas, P. (2017). $\text{BaCe}_{0.5}\text{Zr}_{0.3}\text{Y}_{0.2-x}\text{Yb}_x\text{O}_{3-\delta}$ proton-conducting electrolytes for intermediate-temperature solid oxide fuel cells. *Electrochim. Acta* 251, 554–561. <https://doi.org/10.1016/j.electacta.2017.08.149>.
75. Ma, J., Tao, Z., Kou, H., Fronzi, M., and Bi, L. (2020). Evaluating the effect of Pr-doping on the performance of strontium-doped lanthanum ferrite cathodes for protonic SOFCs. *Ceram. Int.* 46, 4000–4005. <https://doi.org/10.1016/j.ceramint.2019.10.017>.
76. Weber, A. (2021). Impedance analysis of porous electrode structures in batteries and fuel cells. *TM Techn. Mess.* 88, 1–16. <https://doi.org/10.1515/teme-2020-0084>.
77. Williams, N.J., Osborne, C., Seymour, I.D., Bazant, M.Z., and Skinner, S.J. (2023). Application of finite Gaussian process distribution of relaxation times on SOFC electrodes. *Electrochim. Commun.* 149, 107458. <https://doi.org/10.1016/j.elecom.2023.107458>.

78. Li, Y., Jiang, Y., Dang, J., Deng, X., Liu, B., Ma, J., Yang, F., Ouyang, M., and Shen, X. (2023). Application of distribution of relaxation times method in polymer electrolyte membrane water electrolyzer. *Chem. Eng. J.* 451, 138327. <https://doi.org/10.1016/j.cej.2022.138327>.
79. Cholewiak, S., Ipeirotis, P., Silva, V., and Kannanwadi, A. (2021). SCHOLARLY: Simple access to Google scholar authors and citation using Python. *Zenodo*. <https://doi.org/10.5281/zenodo.5764801>.
80. Ciucci, F., Maradesa, A., and Wang, Y. (2024). DRT-Survey. GitHub. <https://github.com/ciuccislab/DRT-Survey>.
81. Liu, J., and Ciucci, F. (2020). The Gaussian process distribution of relaxation times: A machine learning tool for the analysis and prediction of electrochemical impedance spectroscopy data. *Electrochim. Acta* 331, 135316. <https://doi.org/10.1016/j.electacta.2019.135316>.
82. Calvetti, D., and Somersalo, E. (2018). Inverse problems: From regularization to Bayesian inference. *WIREs Comput. Stat.* 10, e1427. <https://doi.org/10.1002/wics.1427>.
83. Paul, T., Chi, P.W., Wu, P.M., and Wu, M.K. (2021). Computation of distribution of relaxation times by Tikhonov regularization for Li ion batteries: Usage of L-curve method. *Sci. Rep.* 11, 12624. <https://doi.org/10.1038/s41598-021-91871-3>.
84. Gavrilyuk, A.L., Osinkin, D.A., and Bronin, D.I. (2020). On a Variation of the Tikhonov regularization method for calculating the distribution function of relaxation times in impedance spectroscopy. *Electrochim. Acta* 354, 136683. <https://doi.org/10.1016/j.electacta.2020.136683>.
85. Hershkovitz, S., Tomer, S., Baltianski, S., and Tsur, Y. (2011). ISGP: Impedance spectroscopy analysis using evolutionary programming procedure. *ECS Trans.* 33, 67–73. <https://doi.org/10.1149/1.3589186>.
86. Tesler, A.B., Lewin, D.R., Baltianski, S., and Tsur, Y. (2010). Analyzing results of impedance spectroscopy using novel evolutionary programming techniques. *J. Electroceram.* 24, 245–260. <https://doi.org/10.1007/s10832-009-9565-z>.
87. Pereverzev, S.V., Solodky, S.G., Vasylk, V.B., and Žic, M. (2020). Regularized collocation in distribution of diffusion times applied to electrochemical impedance spectroscopy. *Comp. Methods Appl. Math.* 20, 517–530. <https://doi.org/10.1515/cmam-2019-0111>.
88. Žic, M., Vlašić, L., Subotić, V., Pereverzyev, S., Fajfar, I., and Kunaver, M. (2022). Extraction of distribution function of relaxation times by using Levenberg-Marquardt algorithm: A new approach to apply a discretization error free Jacobian matrix. *J. Electrochem. Soc.* 169, 030508. <https://doi.org/10.1149/1945-7111/ac55c9>.
89. Ahvanooy, M.T., Li, Q., Wu, M., and Wang, S. (2019). A survey of genetic programming and its applications. *KSII Trans. Internet Inf. Syst.* 13, 38–60.
90. Hershkovitz, S., Baltianski, S., and Tsur, Y. (2011). Harnessing evolutionary programming for impedance spectroscopy analysis: A case study of mixed ionic-electronic conductors. *Solid State Ionics* 188, 104–109. <https://doi.org/10.1016/j.ssi.2010.10.004>.
91. Bello, A., Laredo, E., and Grimal, M. (1999). Distribution of relaxation times from dielectric spectroscopy using Monte Carlo simulated annealing: Application to α -PVDF. *Phys. Rev. B* 60, 12764–12774. <https://doi.org/10.1103/PhysRevB.60.12764>.
92. Liu, J., and Ciucci, F. (2020). The deep-prior distribution of relaxation times. *J. Electrochem. Soc.* 167, 026506. <https://doi.org/10.1149/1945-7111/ab631a>.
93. Boukamp, B.A. (2015). Fourier transform distribution function of relaxation times; application and limitations. *Electrochim. Acta* 154, 35–46. <https://doi.org/10.1016/j.electacta.2014.12.059>.
94. Liedermann, K. (1994). The calculation of a distribution of relaxation times from the frequency dependence of the real permittivity with the inverse Fourier transformation. *J. Non-Crystal. Solids* 175, 21–30. [https://doi.org/10.1016/0022-3093\(94\)90311-5](https://doi.org/10.1016/0022-3093(94)90311-5).
95. Ciucci, F., and Chen, C. (2015). Analysis of electrochemical impedance spectroscopy data using the distribution of relaxation times: A Bayesian and hierarchical Bayesian approach. *Electrochim. Acta* 167, 439–454. <https://doi.org/10.1016/j.electacta.2015.03.123>.
96. Choi, M., Shin, J., Ji, H., Kim, H., Son, J., Lee, J., Kim, B., Lee, H., and Yoon, K. (2019). Interpretation of impedance spectra of solid oxide fuel cells: L-curve criterion for determination of regularization parameter in distribution function of relaxation times technique. *JOM* 71, 3825–3834.
97. Baral, A.K., and Tsur, Y. (2017). Impedance spectroscopy of Gd-doped ceria analyzed by genetic programming (ISGP) method. *Solid State Ionics* 304, 145–149. <https://doi.org/10.1016/j.ssi.2017.04.003>.
98. Maradesa, A., Py, B., Quattrochi, E., and Ciucci, F. (2022). The probabilistic deconvolution of the distribution of relaxation times with finite Gaussian processes. *Electrochim. Acta* 413, 140119. <https://doi.org/10.1016/j.electacta.2022.140119>.
99. Tuncer, E., and Gubanski, S.M. (2001). On dielectric data analysis. Using the Monte Carlo method to obtain relaxation time distribution and comparing non-linear spectral function fits. *IEEE Trans. Dielect. Electr. Insul.* 8, 310–320. <https://doi.org/10.1109/94.933337>.
100. Paul, T. (2020). Modeling of the impedance data of gadolinia doped ceria based actuators: A distribution function of relaxation times and machine learning approach. *J. Phys. D Appl. Phys.* 53, 415503. <https://doi.org/10.1088/1361-6463/ab9c68>.
101. Effat, M.B., and Ciucci, F. (2017). Bayesian and hierarchical Bayesian based regularization for deconvolving the distribution of relaxation times from electrochemical impedance spectroscopy data. *Electrochim. Acta* 247, 1117–1129. <https://doi.org/10.1016/j.electacta.2017.07.050>.
102. Caveltti, D., Kaipio, J.P., and Somersalo, E. (2006). Aristotelian prior boundary conditions. *Int. J. Math. Comput. Sci.* 1, 63–81.
103. Effendy, S., Song, J., and Bazant, M.Z. (2020). Analysis, design, and generalization of electrochemical impedance spectroscopy (EIS) inversion algorithms. *J. Electrochem. Soc.* 167, 106508. <https://doi.org/10.1149/1945-7111/ab9c82>.
104. Li, X., Ahmadi, M., Collins, L., and Kalinin, S.V. (2019). Deconvolving distribution of relaxation times, resistances and inductance from electrochemical impedance spectroscopy via statistical model selection: Exploiting structural-sparsity regularization and data-driven parameter tuning. *Electrochim. Acta* 313, 570–583. <https://doi.org/10.1016/j.electacta.2019.05.010>.
105. Huang, J.D. (2023). Elucidating electrochemical mechanisms with accelerated characterization and relaxation structure analysis. PhD thesis (Colorado School of Mines). <https://hdl.handle.net/11124/178507>.
106. Honerkamp, J., and Weese, J. (1990). Tikhonov regularization method for ill-posed problems. *Continuum Mech. Thermodyn.* 2, 17–30. <https://doi.org/10.1007/BF01170953>.
107. Andersen, M.S., Dahl, J., Liu, Z., and Vandenberghe, L. (2012). Interior-point methods for large-scale cone programming. In *Optimization for Machine Learning*, S. Sra, S. Nowozin, S.J. Wright, and editors, eds. (MIT Press), pp. 55–83.
108. Levenberg, K. (1944). A method for the solution of certain problems in least squares. *Quart. Appl. Math.* 2, 164–168. <https://doi.org/10.1090/qam/1066>.
109. Marquardt, D.W. (1963). An algorithm for least-squares estimation of non-linear parameters. *SIAM J. Appl. Math.* 11, 431–441. <https://doi.org/10.1137/0111030>.
110. Kulikovsky, A. (2020). PEM fuel cell distribution of relaxation times: A method for the calculation and behavior of an oxygen transport peak. *Phys. Chem. Chem. Phys.* 22, 19131–19138. <https://doi.org/10.1039/d0cp02094j>.
111. Macutkevic, J., Banys, J., and Matulis, A. (2004). Determination of the distribution of the relaxation times from dielectric spectra. *Nonlinear Anal. Model. Control* 9, 75–88. <https://doi.org/10.15388/NA.2004.9.1.15172>.
112. Clematis, D., Ferrari, T., Bertei, A., Asensio, A.M., Carpanese, M.P., Nicollella, C., and Barbucci, A. (2021). On the stabilization and extension of the distribution of relaxation times analysis. *Electrochim. Acta* 391, 138916. <https://doi.org/10.1016/j.electacta.2021.138916>.
113. Schlüter, N., Ernst, S., and Schröder, U. (2019). Finding the optimal regularization parameter in distribution of relaxation times analysis. *ChemElectroChem* 6, 6027–6037. <https://doi.org/10.1002/celc.201901863>.
114. Fuoss, R.M., and Kirkwood, J.G. (1941). Electrical properties of solids. VIII. dipole moments in polyvinyl chloride-diphenyl systems. *J. Am. Chem. Soc.* 63, 319–323.

115. Malik, B., Sanker, K.V., Kroner, R., and Tsur, Y. (2020). Determining the electrochemical oxygen evolution reaction kinetics of $\text{Fe}_3\text{S}_4@\text{Ni}_3\text{S}_2$ using distribution function of relaxation times. *ChemElectroChem* 8, 01410.
116. Sarrut, D., Etxeberria, A., Muñoz, E., Krah, N., and Létang, J.M. (2021). Artificial intelligence for Monte Carlo simulation in medical physics. *Front. Phys.* 9, 738112. <https://doi.org/10.3389/fphy.2021.738112>.
117. Kingma, D.P., and Ba, J.L. (2014). Adam: A method for stochastic optimization. Preprint at arXiv.
118. Bartlett, P.L., Long, P.M., Lugosi, G., and Tsigler, A. (2020). Benign overfitting in linear regression. *Proc. Natl. Acad. Sci. USA* 117, 30063–30070. <https://doi.org/10.1073/pnas.1907378117>.
119. Yang, K., Liu, J., Wang, Y., Shi, X., Wang, J., Lu, Q., Ciucci, F., and Yang, Z. (2022). Machine-learning-assisted prediction of long-term performance degradation on solid oxide fuel cell cathodes induced by chromium poisoning. *J. Mater. Chem. A* 10, 23683–23690. <https://doi.org/10.1039/D2TA03944C>.
120. Rasmussen, C.E., and Williams, C.K.I. (2006). *Gaussian Processes for Machine Learning: Adaptive Computation and Machine Learning* (MIT Press).
121. Deringer, V.L., Bartók, A.P., Bernstein, N., Wilkins, D.M., Ceriotti, M., and Csányi, G. (2021). Gaussian process regression for materials and molecules. *Chem. Rev.* 121, 10073–10141. <https://doi.org/10.1021/acs.chemrev.1c00022>.
122. Ziatdinov, M.A., Ghosh, A., and Kalinin, S.V. (2022). Physics makes the difference: Bayesian optimization and active learning via augmented Gaussian process. *Mach. Learn.: Sci. Technol.* 3, 015003. <https://doi.org/10.1088/2632-2153/ac4baa>.
123. Liu, Y., Morozovska, A.N., Eliseev, E.A., Kelley, K.P., Vasudevan, R., Ziatdinov, M., and Kalinin, S.V. (2023). Autonomous scanning probe microscopy with hypothesis learning: Exploring the physics of domain switching in ferroelectric materials. *Patterns (N Y)* 4, 100704. <https://doi.org/10.1016/j.patter.2023.100704>.
124. Hahn, M., Rosenbach, D., Krimalowski, A., Nazarenus, T., Moos, R., Thelakkat, M., and Danzer, M.A. (2020). Investigating solid polymer and ceramic electrolytes for lithium-ion batteries by means of an extended distribution of relaxation times analysis. *Electrochim. Acta* 344, 136060. <https://doi.org/10.1016/j.electacta.2020.136060>.
125. Danzer, M.A. (2019). Generalized distribution of relaxation times analysis for the characterization of impedance spectra. *Batteries* 5, 53. <https://doi.org/10.3390/batteries5030053>.
126. Plank, C., Rüther, T., Jahn, L., Schamel, M., Schmidt, J.P., Ciucci, F., and Danzer, M.A. (2024). A review on the distribution of relaxation times analysis: A powerful tool for process identification of electrochemical systems. *J. Power Sources* 594, 233845. <https://doi.org/10.1016/j.jpowsour.2023.233845>.
127. Chen, J., Quattrochi, E., Ciucci, F., and Chen, Y. (2023). Charging processes in lithium-oxygen batteries unraveled through the lens of the distribution of relaxation times. *Chem* 9, 2267–2281. <https://doi.org/10.1016/j.chempr.2023.04.022>.
128. Brug, G.J., Van Den Eeden, A.L.G., Sluyters-Rehbach, M., and Sluyters, J.H. (1984). The analysis of electrode impedances complicated by the presence of a constant phase element. *J. Electroanal. Chem. Interfacial Electrochem.* 176, 275–295. [https://doi.org/10.1016/S0022-0728\(84\)80324-1](https://doi.org/10.1016/S0022-0728(84)80324-1).
129. Py, B., Maradesa, A., and Ciucci, F. (2024). From theory to practice: Unlocking the distribution of capacitive times in electrochemical impedance spectroscopy. *Electrochim. Acta* 479, 143741. <https://doi.org/10.1016/j.electacta.2023.143741>.
130. Song, J., and Bazant, M.Z. (2018). Electrochemical impedance imaging via the distribution of diffusion times. *Phys. Rev. Lett.* 120, 116001. <https://doi.org/10.1103/PhysRevLett.120.116001>.
131. Lai, W., and Ciucci, F. (2011). Small-signal apparent diffusion impedance of intercalation battery electrodes. *J. Electrochem. Soc.* 158, A115. <https://doi.org/10.1149/1.3515896>.
132. Levi, M.D., Wang, C., and Aurbach, D. (2004). Two parallel diffusion paths model for interpretation of PITT and EIS responses from non-uniform intercalation electrodes. *J. Electroanal. Chem.* 561, 1–11. <https://doi.org/10.1016/j.jelechem.2003.07.014>.
133. Quattrochi, E., Wan, T.H., Curcio, A., Pepe, S., Effat, M.B., and Ciucci, F. (2019). A general model for the impedance of batteries and supercapacitors: The non-linear distribution of diffusion times. *Electrochim. Acta* 324, 134853. <https://doi.org/10.1016/j.electacta.2019.134853>.
134. Schiller, C.A., Richter, F., Gültzow, E., and Wagner, N. (2001). Relaxation impedance as a model for the deactivation mechanism of fuel cells due to carbon monoxide poisoning. *Phys. Chem. Chem. Phys.* 3, 2113–2116. <https://doi.org/10.1039/b007674k>.
135. Hensle, N., Brinker, D., Metz, S., Smolinka, T., and Weber, A. (2023). On the role of inductive loops at low frequencies in PEM electrolysis. *Electrochim. Commun.* 155, 107585. <https://doi.org/10.1016/j.elecom.2023.107585>.
136. Klotz, D. (2019). Negative capacitance or inductive loop? – a general assessment of a common low frequency impedance feature. *Electrochim. Commun.* 98, 58–62. <https://doi.org/10.1016/j.elecom.2018.11.017>.
137. Schiefer, A., Heinemann, M., and Weber, A. (2020). Inductive low-frequency processes in PEMFC-impedance spectra. *Fuel Cells* 20, 499–506. <https://doi.org/10.1002/fuce.201900212>.
138. King, F.W. (2009). *Hilbert Transform* (Cambridge University Press), p. 1.
139. Schönleber, M., Klotz, D., and Ivers-Tiffée, E. (2014). A method for improving the robustness of linear Kramers-Kronig validity tests. *Electrochim. Acta* 131, 20–27. <https://doi.org/10.1016/j.electacta.2014.01.034>.
140. Ciucci, F. (2013). Revisiting parameter identification in electrochemical impedance spectroscopy: Weighted least squares and optimal experimental design. *Electrochim. Acta* 87, 532–545. <https://doi.org/10.1016/j.electacta.2012.09.073>.
141. Boukamp, B.A. (1986). A nonlinear least squares fit procedure for analysis of immittance data of electrochemical systems. *Solid State Ionics* 20, 31–44. [https://doi.org/10.1016/0167-2738\(86\)90031-7](https://doi.org/10.1016/0167-2738(86)90031-7).
142. Boukamp, B.A. (1986). A package for impedance/admittance data analysis. *Solid State Ionics* 18–19, 136–140. [https://doi.org/10.1016/0167-2738\(86\)90100-1](https://doi.org/10.1016/0167-2738(86)90100-1).
143. Liu, J., Wan, T.H., and Ciucci, F. (2020). A Bayesian view on the Hilbert transform and the Kramers-Kronig transform of electrochemical impedance data: Probabilistic estimates and quality scores. *Electrochim. Acta* 357, 136864. <https://doi.org/10.1016/j.electacta.2020.136864>.
144. Pedregosa, F., et al. (2011). Scikit-learn: Machine learning in Python. *J. Mach. Learn. Res.* 12, 2820–2830.
145. Micheal, C.F. (2015). *Handbook of Simulation Optimization*. In International Series in Operations Research & Management, 216International Series in Operations Research & Management (Springer).
146. Parzen, E., Tanabe, K., and Kitagawa, G. (1998). Selected Papers of Hirotugu Akaike. In *Series in StatisticsSeries in Statistics* (Springer).
147. Narayananchari, K.V.L.V., Buchholz, D.B., Goldfine, E.A., Wenderott, J.K., Haile, S.M., and Bedzyk, M.J. (2020). 2. Combinatorial approach for single-crystalline TaON growth: Epitaxial β -TaON (100)/ α -Al₂O₃. *ACS Appl. Electron. Mater.* 012, 3571–3576.
148. Rastegarpanah, A., Ahmeid, M., Marturi, N., Attidekou, P.S., Musbahu, M., Ner, R., Lambert, S., and Stolkin, R. (2021). Towards robotizing the processes of testing lithium-ion batteries. *Proc. Inst. Mech. Eng. Part I J. Syst. Control Eng.* 235, 1309–1325. <https://doi.org/10.1177/0959651821998599>.
149. Koster, D., Du, G., Battistel, A., and La Mantia, F.L. (2017). Dynamic impedance spectroscopy using dynamic multi-frequency analysis: A theoretical and experimental investigation. *Electrochim. Acta* 246, 553–563. <https://doi.org/10.1016/j.electacta.2017.06.060>.
150. Buteau, S., and Dahn, J.R. (2019). Analysis of thousands of electrochemical impedance spectra of lithium-ion cells through a machine learning inverse model. *J. Electrochim. Soc.* 166, A1611–A1622. <https://doi.org/10.1149/2.1051908jes>.
151. Schaeffer, J., Gasper, P., Garcia-Tamayo, E., Gasper, R., Adachi, M., Pablo Gaviria-Cardona, J., Montoya-Bedoya, S., Bhutani, A., Schiek, A., Goodall, R., et al. (2023). Machine learning benchmarks for the classification of equivalent circuit models from electrochemical impedance spectra. *J. Electrochim. Soc.* 170, 060512. <https://doi.org/10.1149/1945-7111/acdbfb>.
152. Bondarenko, A.S. (2012). Analysis of large experimental datasets in electrochemical

- impedance spectroscopy. *Anal. Chim. Acta* 743, 41–50. <https://doi.org/10.1016/j.aca.2012.06.055>.
153. Gramacy, R.B. (2020). *Surrogates: Gaussian Process Modeling, Design, and Optimization for the Applied Sciences* (Chapman and Hall Publishing).
154. Py, B., Maradesa, A., and Ciucci, F. (2023). Gaussian processes for the analysis of electrochemical impedance spectroscopy data: Prediction, filtering, and active learning. *Electrochim. Acta* 439, 141688. <https://doi.org/10.1016/j.electacta.2022.141688>.
155. Ciucci, F., Carraro, T., Chueh, W.C., and Lai, W. (2011). Reducing error and measurement time in impedance spectroscopy using model based optimal experimental design. *Electrochim. Acta* 56, 5416–5434. <https://doi.org/10.1016/j.electacta.2011.02.098>.
156. Sucar, L.E. (2015). *Probabilistic Graphical Models 10* (Springer), p. 1.
157. Oz, A., Gelman, D., Goren, E., Shomrat, N., Baltianski, S., and Tsur, Y. (2017). A Novel Approach for supercapacitors degradation characterization. *J. Power Sources* 355, 74–82. <https://doi.org/10.1016/j.jpowsour.2017.04.048>.
158. Wenzel, M., and Wiegand, T. (2020). Toward global validation standards for health AI. *IEEE Commun. Stand. Mag.* 4, 64–69. <https://doi.org/10.1109/MCOMSTD.001.2000006>.
159. Deng, J., Dong, W., Socher, R., Li, L.-J., Li, K., and Fei-Fei, L. (2009). Imagenet: A large-scale hierarchical image database. In *IEEE Conference on Computer Vision and Pattern Recognition*, pp. 248–255. <https://doi.org/10.1109/CVPR.2009.5206848>.
160. Kavita, G., and ChengXiang, Z. (2012). Opinion-based entity ranking. *Inf. Retrieval* 15, 116–150.
161. Paszke, A., Gross, S., Chintala, S., Chanan, G., Yang, E., DeVito, Z., Lin, Z., Desmaison, A., Antiga, L., and Lerer, A. (2017). Automatic differentiation in PyTorch. 31st Conference on Neural Information Processing Systems.
162. Jordan, M.I., and Mitchell, T.M. (2015). Machine learning: Trends, perspectives, and prospects. *Science* 349, 255–260. <https://doi.org/10.1126/science.aaa8415>.
163. Ciucci, F. (2024). DRTtools: An intuitive GUI for computing DRT based on Tikhonov regularization. GitHub. <https://github.com/ciuccislab/DRTtools>.
164. Ciucci, F. (2024). pyDRTtools: An intuitive GUI for computing DRT based on Tikhonov regularization. GitHub. <https://github.com/ciuccislab/pyDRTtools>.
165. Žic, M. (2023). DRT-RBLM software. <https://sites.google.com/view/drt-rblm-software/home> 2023.
166. Yrjänä, V. (2022). DearEIS: A GUI program for analyzing, simulating, and visualizing impedance spectra. GitHub. <https://vyrjana.github.io/Deareis/>.
167. Macdonald, J.R. (2015). LEVM/LEVMW. <https://jrossmacdonald.com/levmlevmw/>.
168. Žic, M. (2021). DRT-GELM software v.1.01. <https://Bit.Ly/3xkHIUC>.